CAPITAL UNIVERSITY OF SCIENCE AND TECHNOLOGY, ISLAMABAD

Hydro-Thermal Performance of Microchannel Heat Sink Using I-Shaped Pin Fins

by

Hussain Sallar

A thesis submitted in partial fulfillment for the degree of Master of Science

in the

Faculty of Engineering
Department of Mechanical Engineering

2024

Copyright © 2024 by Hussain Sallar

All rights reserved. No part of this thesis may be reproduced, distributed, or transmitted in any form or by any means, including photocopying, recording, or other electronic or mechanical methods, by any information storage and retrieval system without the prior written permission of the author.

I would like to dedicate this thesis to my Parents and my Supervisor,

Dr.Muhammad Irfan for helping me achieve this milestone.

CERTIFICATE OF APPROVAL

Hydro-Thermal Performance of Microchannel Heat Sink Using I-Shaped Pin Fins

by

Hussain Sallar

(MME213003)

THESIS EXAMINING COMMITTEE

S. No.	Examiner	Name	Organization
(a)	External Examiner	Dr. Muhammad Anwar	IST, Islamabad
(b)	Internal Examiner	Dr. M. Mahabat Khan	CUST, Islamabad
(c)	Supervisor	Dr. Muhammad Irfan	CUST, Islamabad

Dr. Muhammad Irfan
Thesis Supervisor
May, 2024

Dr. M. Mahabat Khan
Head
Dept. of Mechanical Engineering
May, 2024

Dr. Imtiaz Ahmad Taj
Dean
Faculty of Engineering
May, 2024

Author's Declaration

I, **Hussain Sallar** hereby state that my MS thesis titled "**Hydro-Thermal Performance of Microchannel Heat Sink Using I-Shaped Pin Fins** " is my own work and has not been submitted previously by me for taking any degree from Capital University of Science and Technology, Islamabad or anywhere else in the country/abroad.

At any time if my statement is found to be incorrect even after my graduation, the University has the right to withdraw my MS Degree.

(Hussain Sallar)

Registration No: MME213003

Plagiarism Undertaking

I solemnly declare that research work presented in this thesis titled "**Hydro-Thermal Performance of Microchannel Heat Sink Using I-Shaped Pin Fins** " is solely my research work with no significant contribution from any other person. Small contribution/help wherever taken has been duly acknowledged and that complete thesis has been written by me.

I understand the zero tolerance policy of the HEC and Capital University of Science and Technology towards plagiarism. Therefore, I as an author of the above titled thesis declare that no portion of my thesis has been plagiarized and any material used as reference is properly referred/cited.

I undertake that if I am found guilty of any formal plagiarism in the above titled thesis even after award of MS Degree, the University reserves the right to withdraw/revoke my MS degree and that HEC and the University have the right to publish my name on the HEC/University website on which names of students are placed who submitted plagiarized work.

(Hussain Sallar)

Registration No: MME213003

Acknowledgement

I would like to thank God Almighty for giving me an opportunity to undertake this task. I would further like to thank my Parents and my thesis Supervisor, Dr. Muhammad Irfan for helping me immensely, in completion of this task. I am obliged to Dr. Mahabt Khan , Head of Department, Mechanical Engineering, CUST, for giving me access to high performance Computer Servers for carrying out multiple time consuming Numerical Simulations.

(Hussain Sallar)

Abstract

I-shaped pin fin microchannel heat sinks have been investigated numerically in order to determine heat transfer and fluid flow behavior. Pin fin height and thickness are varied from 0.75-2 mm and 0.1-0.4 mm, respectively. Single phase liquid water is taken as working fluid of the microchannel heat sink. Base temperature, Nusselt number, pressure drop and thermal performance factor are key performance parameters. Initial simulations are carried out at Reynolds number of 800 and heat flux of 150 kW/m^2 and an optimum case is identified having fin height of 1.5 mm and thickness of 0.4 mm. Optimum case has a thermal performance factor of 1.16. For the optimum case, simulations are carried out by varying Reynolds number from 200-800 while heat flux value from 75-150 kW/m^2. Results indicate that as fin height and thickness increase, thermal performance of the heat sink is enhanced. In addition, hydraulic performance based on the pressure drop is decreased with an increase in fin height and thickness. Hydro-thermal performance is dominated by fluid flow characteristics within a heat sink. Coolant recirculation behind pin fins gives rise to mixing effects which leads to better thermal performance. Availability of open space in the heat sink contributes positively towards heat transfer. In this context, a completely closed heat sink having fin height of 2 mm has lower hydro-thermal performance relatively. In order to enhance hydro-thermal performance, pin fins are oriented at orientations of 15° to 90° and four angled geometric configurations are created. Results indicate that Configuration-3 at 15° has the highest thermal performance factor of 1.29. This corresponds to an increase in performance of 29%. Fluid flow characteristics for angled cases are distinct and unique. Converging and diverging channels are created as pin fin orientation and geometric configurations are varied. This gives rise to distinct velocity profiles which dictate the hydro-thermal performance.

Contents

Author's Declaration iv

Plagiarism Undertaking v

Acknowledgement vi

Abstract vii

List of Figures x

List of Tables xii

Abbreviations xiii

Symbols xiv

1 Introduction 1
- 1.1 Motivation . . . 2
- 1.2 Problem Statement . . . 3
- 1.3 Objectives . . . 4
- 1.4 Advantages . . . 4
- 1.5 Applications . . . 4
- 1.6 Report Structure . . . 5

2 Literature Review 6
- 2.1 Novelty of the Design . . . 19

3 Problem Formulation 20
- 3.1 Geometrical Modelling . . . 20
- 3.2 Solution Methodology . . . 21
  - 3.2.1 Governing Equations . . . 23
  - 3.2.2 Fluid Properties . . . 23
  - 3.2.3 Boundary Conditions . . . 24
  - 3.2.4 Numerical Methods . . . 24
  - 3.2.5 Grid Generation and Grid Independence . . . 26
  - 3.2.6 Performance Parameters . . . 28
  - 3.2.7 Validation Study . . . 30

4 Effects of Fin Height and Thickness on Hydro-Thermal Performance 32
4.1 Surface Area and Cross-sectional Shape Sizes of Pin Fins 33
4.2 Performance Parameters v/s Thickness for Different Fin Heights H . 35
4.3 Velocity Contours at X=0.4 mm for Varying Fin Heights 37
4.4 Temperature Contours:X=0.4 mm for Varying Fin Heights 39
4.5 Performance Parameters vs Reynolds number for Varying Heat Flux 41
4.6 Effects of Varying Reynolds Number on Velocity Contours 43
4.7 Effects of Varying Reynolds Number: Temperature Contours 45
4.8 Effects of Varying Heat Flux on Temperature Contours 46
4.9 Velocity Streamlines 47
4.10 Thermal Resistance 48

5 Effects of Fin Orientation on Hydro-Thermal Performance 51
5.1 Geometry 52
5.2 Mesh 53
5.3 Performance Parameters v/s Angle 'θ' 54
5.4 Configuration-3 -Velocity Contours at Orientations of 15°-90° 56
5.5 Configuration-3 -Temperature Contours at Orientations of 15°-90° . 58
5.6 15°-Velocity Contours for All Configurations 59
5.7 15°-Temperature Contours for All Configurations 61
5.8 75°-Velocity Contours for All Configurations 62
5.9 75°-Temperature Contours for All Configurations 64

6 Conclusion and Future Work 66
6.1 Future Recommendations 67

Bibliography 69

List of Figures

1.1 Cooling methods and their classification[Reprinted from [2]] 2
1.2 Evolution of maximum chip heat flux, power and transistor count over the past two decades[Reprinted from [2]] 3
1.3 (a) Pentium 4 heat sink with fan, (b) Schematic of the heat sink (c) Thermal resistance circuit[Reprinted from [7]] 5

2.1 Causes of failure in electronic devices[Reprinted from [8]] 6
2.2 Techniques for heat transfer enhancement in microchannel heat sinks[Reprinted from [9]] 7

3.1 Geometry of the heat sink (a) cross sectional view (b) isometric view (c) top view (d) cross section of a single I-shaped pin fin . . . 22
3.2 Schematic diagram representing boundary conditions on the geometry 25
3.3 Mesh (a) isometric view, (b) cross-sectional view, (c) pin fin cross-section 27
3.4 Grid independence based on pressure drop, ΔP 28
3.5 Representation of A_{csa} and A_{bw} 30
3.6 Validation study (a) base temperature vs Reynolds number (b) pressure drop vs Reynolds number 31

4.1 Surface area and cross-sectional shape sizes of pin fins 34
4.2 (a) Base temperature, (b) Nusselt number, (c) pressure drop, (d) TPF against varying fin thickness for all the fin heights 35
4.3 Velocity contours at X=0.4 mm for varying fin heights 37
4.4 Temperature contours at X=0.4 mm for varying fin heights 40
4.5 (a) Base temperature, (b) Nusselt Number, (c) pressure drop and (d) TPF vs Reynolds for changing heat flux for fin height of 1.5 mm and thickness of 0.4 mm 42
4.6 Velocity contours for varying Reynolds number 44
4.7 Temperature contours for varying Reynolds number 45
4.8 Temperature contours for varying heat flux 46
4.9 Velocity streamlines for fin heights of 1 mm and 1.75 mm 48
4.10 Thermal resistance against fin thickness for varying fin heights . . . 49

5.1 Geometry representing angled cases, (a) Configuration-1, (b) Configuration-2, (c) Configuration-3, (d) Configuration-4, at θ= 30° 52
5.2 Representation of mesh for angled cases, (a) isometric view, (b) heat sink cross-section, (c) pin fin cross section 53

5.3 Performance parameters v/s Angle 'θ', (a) base temperature, (b) Nusselt Number, (c) pressure drop and (d) TPF 54
5.4 Velocity contours at multiple orientations for Configuration-3 57
5.5 Temperature Contours at multiple orientations for C-3 59
5.6 Velocity contours for all configurations at 15° 60
5.7 Temperature contours for all configurations at 15° 62
5.8 Velocity contours for all configurations at 75° 63
5.9 Temperature contours for all configurations at 75° 65

List of Tables

3.1 Geometrical parameters 21
3.2 Mesh types based on element size 26

4.1 Simulated cases 33

Abbreviations

C-X	Configuration-1,2,3..
ICs	Integrated Circuits
LED	Light Emitting Diode
MCHS	Microchannel heat sink
Opt	Optimum Case

Symbols

H	Fin height
X	Fin thickness
T_b	Base temperature
Nu	Nusselt number
ΔP	Pressure drop
ψ	Thermal performance factor
θ	Angular orientation
D_h	Hydraulic diameter
A_{csa}	Contact surface area
A_{bw}	Bottom wall surface area
q_{eff}	Effective heat flux
h	heat transfer coefficient

Chapter 1

Introduction

The utility of integrated circuits (ICs) was first established in 1949 by Werner Jacobi [1]. Since then, integrated circuits have evolved continuously in size and performance. In an electronic circuit, components of an integrated circuit draw current due to which heat is generated. In this context, cooling of ICs is of a paramount importance. Various cooling methods have been adopted for this purpose. These cooling methods are categorized on the basis of contact of electronic device with the working fluid. Direct and Indirect contact methods are two primary methods of cooling [2]. Direct contact cooling involves techniques like air cooling, spray cooling, jet impingement etc. Indirect cooling involves techniques like microchannel heat sink cooling, PCM (Phase Change Material) cooling, thermoelectric cooling etc. Figure 1.1 presents a classification of cooling methods employed in cooling of electronic devices.

Microchannel heat sinks (MCHS) are cooling devices that have their maximum dimensions in the order of millimeters. In 1981, Tuckerman and Pease pioneered the concept of microchannel heat sinks [3]. Tuckerman and Pease wanted to design a compact heat sink for high power integrated circuits that were being developed. Experimental work was conducted and it was concluded that the coolant viscosity is the driving force to determine the microchannel width. It was found that channel width has inverse relationship with convective heat transfer coefficient 'h'. Thus, in conclusion microchannel heat sinks are not only compact but also efficient. Furthermore, water was used as the coolant and experiments were conducted only

for laminar flow. This cooling method allowed the IC to operate at 71°C against heat flux of 790 W/cm^2. At that time this power rating was very high for electronic circuits.

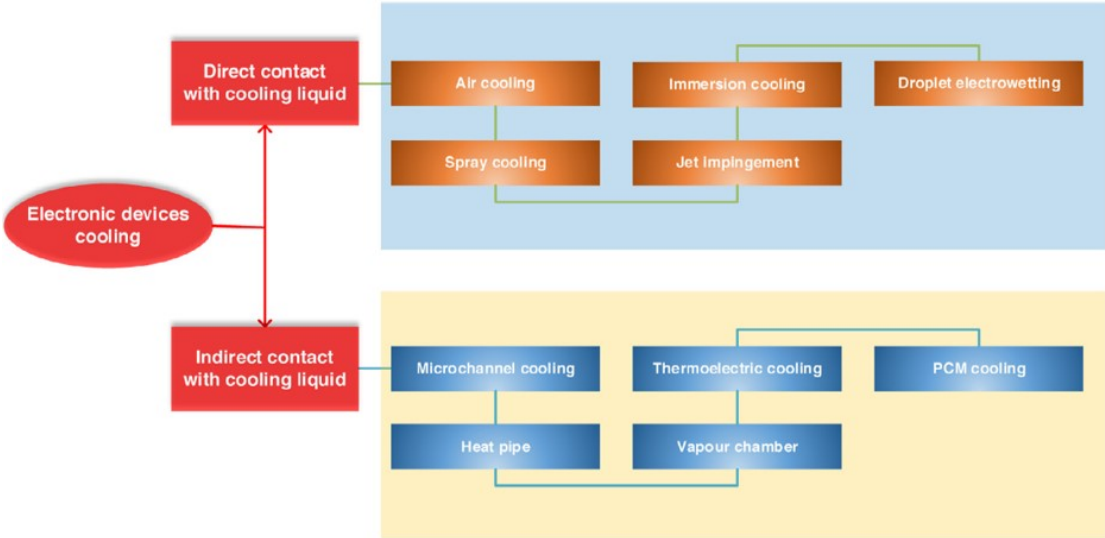

FIGURE 1.1: Cooling methods and their classification[Reprinted from [2]]

1.1 Motivation

Microprocessors can run safely between 80°C to 100°C but their optimum operating temperature is 60°C [4]. With the passage of time, number of transistors have increased in the integrated circuits. Higher the number of transistors in an integrated circuit, higher the computing power. To increase the number of transistors, transistor size is decreased in the orders of nano meters. Figure 1.2 presents the evolution of maximum chip heat flux, maximum power and transistor count over the past two decades. The importance of conjugate heat transfer problems and their solutions derived from numerical modelling is also a driving force for this study. Forced convection has always been a preferred way for heat transfer in many applications including MCHS. It is of paramount importance to apply numerical methods for solving heat transfer problems of this nature. Furthermore, there exists a huge potential in scope of improvement in the design of microchannel heat sinks. Design of MCHS can be improved by manipulating different parameters, namely shape of fins, geometric parameters of the fins, arrangement of the fins,

density of the fins, working fluid etc. It is because of these reasons; research work has been carried out on this topic till this day.

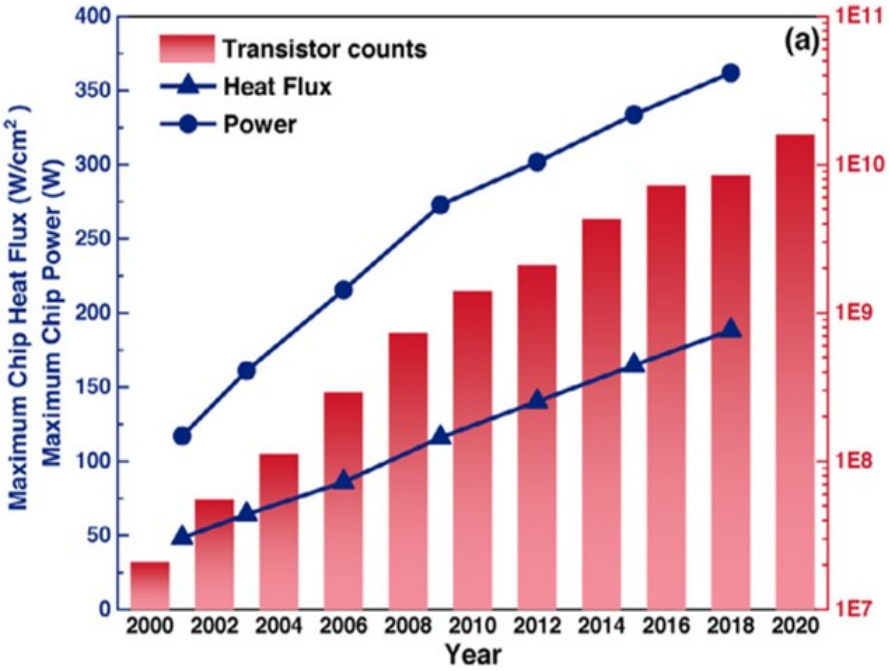

FIGURE 1.2: Evolution of maximum chip heat flux, power and transistor count over the past two decades[Reprinted from [2]]

The motivation of this study revolves around the concept of potential of maximum heat dissipation through a compact cooling device. Pin fin microchannel heat sinks are compact cooling devices that offer a substantial amount of heat dissipation. With the development of high-power electronic devices, the need to cool them has also arisen. Since these devices draw a lot of current, they need to be cooled properly.

1.2 Problem Statement

Microchannel heat sinks are important engineering devices used to transfer heat and cool integrated circuits (ICs). It is therefore important to analyze their performance in the context of geometrical changes. The problem statement of this research work is as follows,

Numerical analysis of an I-shaped pin fin microchannel heat sink to determine and enhance it's hydro-thermal performance.

1.3 Objectives

The primary objective of this study is to enhance the hydro-thermal performance of an I-shaped pin fin microchannel heat sink by varying its geometrical parameters. Furthermore, understanding flow physics around an I-shaped pin fin is also of importance.

1.4 Advantages

The advantages of MCHS were realized when computing power of electronic components increased, in the late 20th century. One of their main advantage is higher heat dissipation despite of their compact size. According to Asish et al. [5], microchannel heat sinks have very high surface area to volume ratio due to which they provide much larger rates of heat dissipation, when compared to conventional heat sinks. Due to compactness, MCHS have less weight and occupy less space. In this context, available space and weight are very important parameters especially in the field of aviation.

1.5 Applications

Microchannel heat sinks are employed in computer processors, graphic cards, LED light bulbs etc. They are also widely used in electronics related to defense industry. Processing speed of computers is increasing with each passing year and will continue to increase in the coming decades. In late 1990's and early 2000's, consumer grade computers were becoming increasingly common in markets. According to Intel, Pentium 4 processor was introduced in 2002 which provided 450 million people worldwide an opportunity to operate processors at 2.2 GHz instead of 700 Mhz [6]. Introduction of this processor was a milestone event in the history of computers. For heat transfer and cooling, Pentium 4 processor employed a heat sink with a cooling fan on top. Figure 1.3 presents a (a)Pentium 4 processor, (b) it's schematic diagram and (c) it's thermal resistance circuit diagram [7].

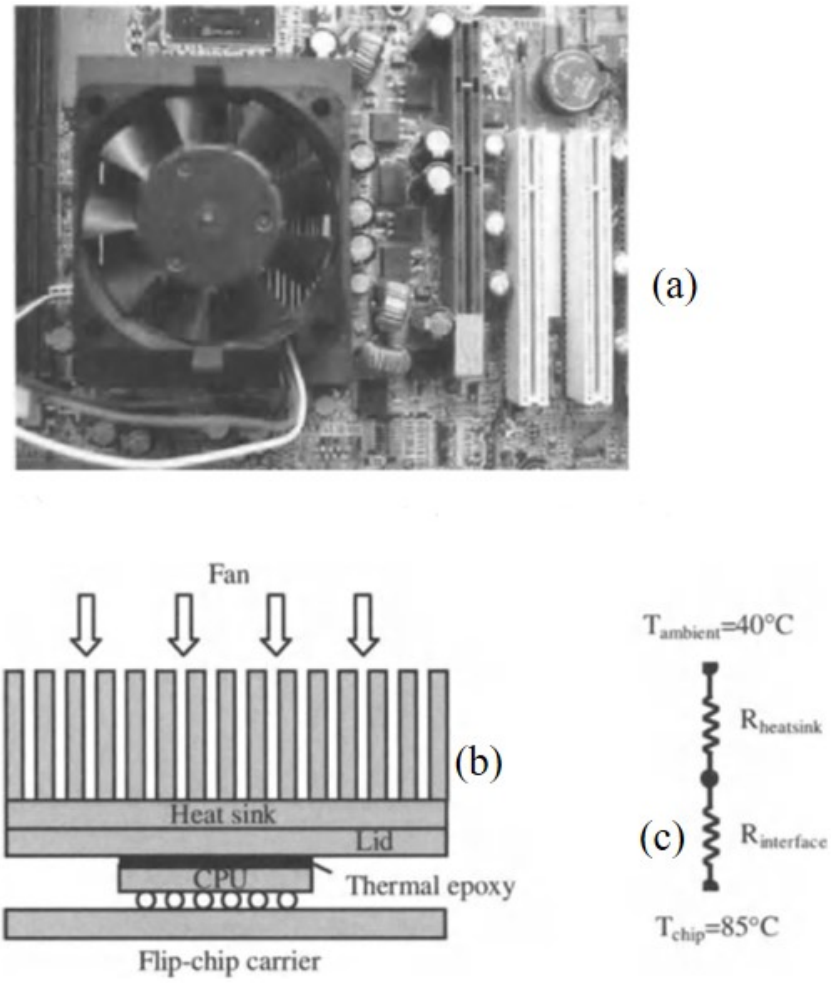

FIGURE 1.3: (a) Pentium 4 heat sink with fan, (b) Schematic of the heat sink (c) Thermal resistance circuit[Reprinted from [7]]

1.6 Report Structure

This report is made up of 6 chapters. Chapter 1 is the introductory section of the report. A comprehensive literature review is carried out in chapter 2. Chapter 3 formulates the research problem with inclusion of details regarding heat sink geometry, governing equations, boundary conditions etc. Chapter 4 covers the results and discussion section. Performance parameters are plotted and respective contours are created for analysis. Chapter 5 is based on angled geometric cases. Multiple pin fin orientations are considered along with 4 different pin fin configurations. Performance parameters are plotted along with supporting contours of temperature and velocity. Chapter 6 concludes the report and future recommendations are given for further research.

Chapter 2

Literature Review

Heat sinks are cooling devices that dissipate excess heat from a heat source. Excess heat is directly related to failures in numerous engineering systems/environments. Any device that dissipates heat is considered as a heat sink. Heat sinks are used on engine blocks, electric motor casings, rifle barrels, electronic devices etc. Electronic devices make excessive use of integrated circuits. Electronic devices are prone to failures due to excess heat. According to Tong et al., failure in electronic devices due to excess temperature amounts to 55% [8]. Figure 2.1 presents different causes of failures in electronic devices. Temperature, vibrations, humidity and dust are the major contributors.

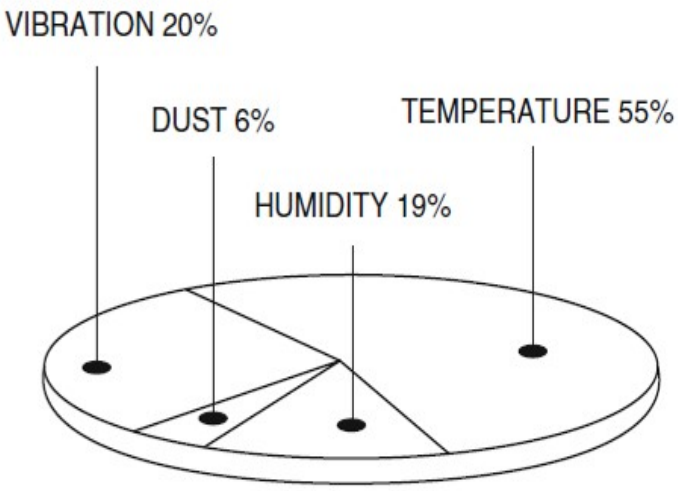

FIGURE 2.1: Causes of failure in electronic devices[Reprinted from [8]]

The need for MCHS emerged as integrated circuits became smaller with the passage of time. Microprocessors which are made up of integrated circuits, are used in majority of electronic appliances. Microprocessors are required to perform millions of calculations per second. Use of microprocessors in electromechanical systems is steadily increasing with the passage of time. Furthermore, electro-mechanical systems and machines are excessively used in various industries like, manufacturing, aviation, agriculture etc. In this context, cooling devices like MCHS have become an essential need for proper operation of these engineering systems.

Heat transfer enhancement in MCHS can be achieved using different techniques. These techniques include, geometric modification, working fluid modification, boiling and evaporation of the working fluid etc. Each of the afore mentioned techniques are divided into further categories. According to Bandari et al., different techniques are used to enhance heat transfer in MCHS [9]. Figure 2.2 presents different techniques which are used to enhance heat transfer in MCHS.

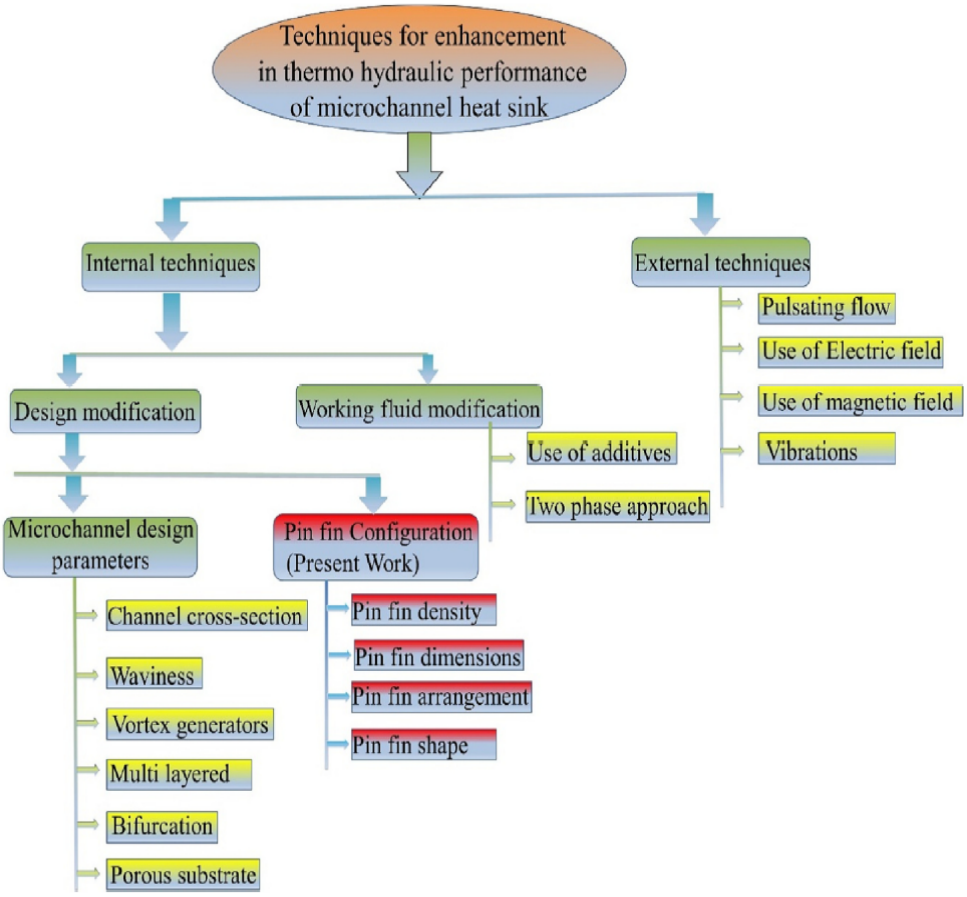

FIGURE 2.2: Techniques for heat transfer enhancement in microchannel heat sinks[Reprinted from [9]]

Throughout the course of development of microchannel heat sinks, researchers have tried to optimize geometry to achieve desired optimal results. Since heat transfer depends heavily on surface area, optimization of surface area had been and will be an active research area. This current research is also based on selection of innovative shapes based on the concept of maximizing surface area. In 1998, Perret et al. [10] performed computational studies to compare different cross sections namely rectangular, diamond shape and hexagon shape for a MCHS. Results showed that rectangular cross section heat sink had the lowest value of thermal resistance i.e 0.16 K/W/cm^2. Similarly, Wang et al. [11] carried out a numerical study to find an optimum cross section for MCHS among rectangular, triangular and trapezoidal geometry. The conclusion being that the rectangular cross section showed the best thermal performance among all three. The rectangular cross section encountered a lowest thermal resistance value of 7 K/W at Reynolds number of 800. Furthermore, it was concluded that thermal and hydraulic performance are a function of number of channels in the heat sink. Number of channels have a direct relation with thermal performance while having an indirect relation with pressure drop. The optimum numerical value for the number of channels of a MCHS is 48-66 channels.

Alfaryjat et al. [12] conducted a numerical investigation to find out the best cross section among hexagonal, rhombus and circular geometrical shape. It was determined that hexagonal cross section had the highest heat transfer coefficient of 26.8 kW/m^2-K at Reynolds number of 1000. Furthermore, hexagonal cross section also had the highest pressure drop of 31.2 kPa. In addition, in terms of friction factor and thermal resistance, rhombus cross section had the least values of the both parameters i.e 0.03 and 0.05 K/kW/m^2 respectively.

Researchers have frequently employed different techniques to enhance heat transfer for example addition of ribs. In 2006, Wang et al. [13] numerically investigated tree shaped channels for microchannel heat sinks and suggested that the type is best suited for uniformity of temperature distribution and anti-blockage effects while having drawbacks as 10% increase in pressure drop value and difficulty in the perceived manufacturing process. In 2010, Xia et al. [14] numerically studied the effects of reentrant triangular cavities on the thermal hydraulic performance of

a MCHS. It was determined that the rate of heat transfer was enhanced using this technique due a number of reasons among which formation of vortices in the cavity and the presence of a thermal boundary layer. Furthermore, different geometrical parameters of the cavity were optimized for better heat transfer enhancement.

Zhu et al. performed a numerical study to determine heat transfer characteristics for different geometric configurations [15]. Microchannel heat sinks with rectangular grooves and different rib shapes were investigated. The rib shapes included four different variations named forward triangular, elliptical, diamond and rectangular. Inclusion of ribs induce flow disturbances which enhance heat transfer. The results showed that for Reynolds number less than 500, rectangular ribs perform best, for Reynolds number less than 700, elliptical ribs perform best and for Reynolds number greater than 700, diamond ribs perform best. So, in conclusion, generalizing performance of a rib shape for all conditions is not possible since Reynolds number plays a critical role in heat transfer. Zhuang et al. [16] carried out a study on a MCHS with rhombus fractal shapes. It was determined that when comparing with conventional parallel channel heat sinks, the heat sink with rhombus fractal shapes increases the coefficient of performance from 7.9% to 68.9%.

In the context of getting enhanced heat transfer through geometric optimization, rectangular microchannel heat sinks have been investigated thoroughly. One aspect of this optimization is to find the optimum number of channels of a heat sink. One can perceive that by increasing the number of channels, heat transfer must be increased. Ramakrishna et al. [17] numerically studied the optimum number of channels for a rectangular MCHS. It was noted that the optimum number of channels are 120 channels per cm. It must be noted that beyond this numerical value of number of channels, heat transfer enhancement is not positively affected. Effects of increase in fin height of a rectangular heat sink was numerically investigated by Prajapati [18]. The author formulated the problem on the basis of increasing the fin heights and finding their effect on heat transfer and pressure drop. With the maximum possible fin height as 1 mm, it was found that 0.8 mm fin height performs best. It was realized that closed heat sinks do not exhibit the optimum performance i.e., a reduction in heat transfer of about 5-10% relative to fin height of 0.8 mm. A general conclusion based on the findings was made that

by increasing that fin height, heat transfer increases along with the pressure drop, in accordance with theoretical observation/inference.

Gamrat et al. [19] performed both 2D and 3D numerical investigations on rectangular MCHS concluding that both 2D and 3D simulations yielded almost comparable results indicating a similarity. In addition to that, entrance effects were studied and it was shown that there was a dependency on Reynolds number and channel spacing. Koşar [20] numerically studied the effects of material thickness and type on the heat transfer of a rectangular heat sink with the objective of developing a correlation of Nusselt number. Porous fins have also been under investigation by the researchers. Chiu et al. [21] investigated both numerically and experimentally the effects of porosity and aspect ratio on heat transfer of MCHS. It was noted that with an increase in the aspect ratio, the local Nusselt number decreased to a minimum value of 0.1. In addition, it was also determined that for a constant pressure drop, Reynolds number decreases to a minimum value of 20, by increasing aspect ratio and porosity.

This study is specifically related to pin fin microchannel heat sinks. A comprehensive literature review regarding pin fin MCHS is required. Abdoli et al. [22] performed 3D numerical simulations on different pin fin shapes and compared them with circular pin fin case. It was reported that flow separation in circular pin fin shapes lead to a higher pressure drop. Results indicated that by using hydrofoil pin fins, pressure drop can be reduced by 30%. Whereas a relatively small increase of heat transfer was also observed. Convex shaped pin fins reduced the pressure drop by around 47%, signaling a huge improvement over circular pin fins. A modified hydrofoil pin fin was also considered which increased heat transfer significantly compared to base case. Ali et al. [23] experimentally studied square pin fin MCHS with two arrangements namely inline and staggered. Working fluids were distilled water and titanium dioxide nanofluids. Results revealed that staggered arrangement performs best as compared to inline arrangement. Furthermore, titanium dioxide nanofluids gave better thermal performance than distilled water.

The effect of varying heat flux/heat load on pin fin MCHS has also been investigated by Guan et al. [24]. The authors conducted an experimental and a numerical

study to conclude that as the heat flux increases, thermophysical properties of the working fluid change which disrupts the boundary layer, decreasing its thickness to 33%. Furthermore, due to an increase in the temperature difference, Nusselt number also increased by 20%. The effect of aspect ratio on heat transfer was also explored. It was found that for smaller aspect ratio pin fin microchannels, Nusselt number was significantly greater compared to the one with larger aspect ratio with percentage difference of around 35%. In the context of increasing heat load, it was noted that the effect of viscosity was larger than thermal conductivity, on heat transfer.

Ansari et al. [25] proposed heat transfer enhancement using a hybrid heat sink. A 3d numerical study was carried out with a hybrid heat sink having rectangular fins for low heat flux region and cylindrical pin fins for a high heat flux region. A comparison was made with a non-hybrid or simple MCHS. It is to be noted that pin fins were only employed in the high heat flux region. It was found that at a Reynolds number of 200, hybrid heat sink maintained 30% less temperature at the expense of 12% increase in pressure drop. At a higher Reynolds number of 800, the hybrid heat sink performed even better. Ansari et al. conducted a numerical study on the same setup except for a stepped cylindrical pin fin arrangement in the high heat flux region [26]. It was realized that the hybrid heat sink with stepped arrangement performed significantly better than non-stepped arrangement, both in terms of thermal and hydraulic performance.

Stepped fins in microchannel heat sinks have been studied by researchers in detail. Bhandari et al. [27] conducted a numerical investigation on stepped pin fin microchannel heat sinks. Seven different configurations were chosen for study i.e from two, three and four stepped increasing to two, three and four stepped decreasing. Square shape was chosen for the cross section of pin fins. Results showed that four stepped decreasing arrangement performed lowest in terms of thermal performance among the stepped fins while performing around 14% better than the base case (uniform pin fin height). It was also found that in context of stepped arrangement, increasing fin height performs better than decreasing fin height. In terms of pressure drop comparison, it was found that increasing pin fin arrangements have higher pressure drop than decreasing pin fin arrangements.

Bhandari et al. performed a numerical investigation on stepped pin fin arrangements in the context of three-dimensional effects and effects of tip clearance [28]. Results indicated that for a 25% tip clearance, thermal performance increased by 8% along with a decrease in pressure drop of 21%. It was also established that stepped arrangement enhances mixing of the working fluid which is favorable for the heat transfer.

Bhandari et al. [29] numerically studied different prism shapes as pin fins for a MCHS. Among the shapes considered were three, four, five, six, seven, eight and nine sided prisms. It was reported that a three-sided prism has lowest while a four-sided prism has the highest thermal performance. Chiu et al. [30] conducted numerical and experimental study on a pin fin MCHS to study the effects of specific geometrical parameters on heat transfer. It was concluded that pin fin porosity and diameter play a crucial role in determining its thermal performance. For instance, pin fins of small diameter provide more surface area for heat transfer. Cooke et al. [31] conducted an experimental investigation for enhancement of pool boiling. Different geometrical parameters were varied and studied to find out their effects. It was found that for the best thermal performance, fins must be thin with a thickness of 200 μm, with a greater depth of 445 μm and in a wide channel of 400 μm.

According to a review paper by Deng et al. [32], there still exists a need to carry out studies to optimize different shapes and passages for heat transfer enhancement of MCHS. Hasan [33] numerically investigated the effects of different pin fin cross sectional shapes and nano fluids in combination. From results it was established that for a constant temperature boundary condition, pin fins with circular cross section have the highest heat transfer while pin fins with square cross section have the highest pressure drop. Hua et al. conducted an experimental study on pin fin microchannel heat sinks with different shapes including, ellipse, circular, diamond, triangular and square [34]. Pin fin density and diameters(equivalent) were also variable parameters. It was found that with an increase in mass flow rate of working fluid, the temperature of the fin base decreases. Furthermore, it was also established that for Reynolds number less than 100, the effect of fin shape on heat transfer is very small.

Hua et al. conducted an experimental investigation to establish the effects of pin fin shape, size and density on pressure drop and friction factor [35]. It was found that pressure drop is directly related to pin fin height and density. The friction coefficient displayed a peculiar relationship with Reynolds number. Below a Reynolds number of 600, an increase in Reynolds caused a rapid decrease in friction factor while for Reynolds number of above 600, this behavior changed. Besides this, it was also found that a circular pin fin produced more flow resistance while an oval shape pin fin produced the least among all the shapes considered. Izci et al. conducted a numerical study on the effects of different pin fin shapes on the hydro-thermal performance of a MCHS for low Reynold numbers (20-120) [36]. It was established that rectangular shape yielded the highest heat transfer coefficient 'h'. The authors reasoned that having multiple sharp points on a pin fin assists in achieving higher heat transfer coefficient, due to flow separation. While rectangular pin fins had highest heat transfer coefficient value, this came at an expense of highest pressure drop among all shapes considered. Cone shape pin fins exhibited the highest thermal performance factor among all shapes considered.

John et al. conducted a numerical study on S-shaped pin fins [37]. It was concluded that S-shaped fins have a higher thermal performance factor compared to other shapes. It was found that S-shape helps in avoiding hotspots i.e areas with higher temperature compared to immediate surroundings. Keshavarz et al. performed a numerical study for drop shaped pin fins with varying geometric parameters, considering aluminum oxide-water and copper oxide-water as working fluids [38]. The varying geometric parameters included fin density and fin arrangements i.e inline and staggered. For inline arrangement, six, nine and fifteen fins represented the fin density. On the other hand, for staggered arrangement, six, eight and fourteen fins represented the fin density. The results were compared with circular pin fins. From numerical results it was found that when compared to circular pin fins, using drop shaped pin fins reduced the pressure drop by 7%. Furthermore, outlet temperature was also increased by 0.6%, depicting an increase in thermal performance.

Sadaghiani and Kosar conducted a numerical analysis to find out best performing pin fin shapes for a MCHS with gas as a working fluid [39]. Results showed

that diamond pin fins perform better in terms of thermal performance relative to rectangular pin fins i.e a difference of 15.9% in the value of Nusselt number. The reason of this finding was attributed to diamond fins having fewer sharp corners, having less obstructing area to the flow and having a tendency to cause mixing relative to the rectangular pin fins. Kewalramani et al. conducted a numerical and experimental study to assess the hydro-thermal performance of a MCHS with elliptical pin fins [40]. It was determined that fin aspect ratio and porosity govern the performance of a heat sink. Optimum values of aspect ratio and porosity were found to be 1.5 and 0.9 respectively.

Aliabadi et al. performed both numerical and experimental analysis to find the performance of a pin fin MCHS with different pin fin shapes along with water and aluminum oxide/water nano fluid as the working fluids [41].The studies were conducted at low Reynolds number range of 100-900. Pin fin shapes comprised of semi-circle, circle, trapezoid, hexagon, triangle, rhombus, rectangle and square. Aluminum/water nanofluid was chosen with two volumetric concentrations of 0.3% and 0.6% and results were compared with water. It was found that each pin fin shape exhibited different vortex formation/recirculation zone leading to different performance. It was also found that the effects of highest vortex formation/recirculation were associated with semi-circle pin fin shape. It was found that relative to square pin fins, semi-circle pin fin achieved 85% more heat transfer at the expense of a pressure drop of 2.5 times. Lee et al. conducted a parametric experimental study to find out the performance of oblique pin fins for a MCHS [42]. Oblique angle and pitch of the fins were parameters governing the optimization. At a Reynolds of 680, a positive heat transfer enhancement of 47% was achieved. Similarly, it was found that for better thermal performance, smaller oblique angle is ideal. Moreover, fin with smaller pitch were also found to be beneficial for thermal performance because of re development of boundary layer.

Kosar et al. conducted an experimental investigation using de ionized water as the working fluid on circular and diamond shaped pin fins with low/small aspect ratio [43].Two configurations were studied namely, staggered and inline. It is important to note that chosen Reynolds number ranged from 5-128. One of the important findings was made regarding the aspect ratio or pin fin height to diameter ratio.

It was found that for a low height to diameter ratio, much higher friction factors are encountered relatively. The research also found that diamond shaped pin fins produced higher values of friction factor relative to circular pin fins. Kosar and Peles performed an experimental investigation on a circular pin fin MCHS to evaluate its thermal and hydraulic performance [44]. It was established that fin wall temperature increases linearly as heat flux is increased. It was also found that end wall effects are prevalent in low Reynolds number flows thus providing a suitable context for deviation of results from existing analytical correlations. The effects of development of boundary layer along with flow separation were also taken in to consideration.

Kosar and Peles conducted an experimental investigation for the aim of parametric optimization of pin fin MCHS [45]. Governing parameters/variables for the optimization were pin fin shape, spacing and arrangement. Low Reynolds number flow in the range of 14-720 was considered with de ionized water as the working fluid. It was found that to enhance heat transfer, large pin fin spacings should be avoided. It was recommended that fins should have less spacing and should have a staggered arrangement instead of inline arrangement. It was also established that a pin fin with sharp region in its geometry is bound to enhance heat transfer than a pin fin having a streamlined or smooth geometry. The reason for this is of course due to flow separation directly related to sharp edges/corners, producing an effect of increased flow mixing. All this enhancement of heat transfer comes at a price of pressure drop which significantly increases when small fin spacing is used along with sharp/pointed edges.

Liu et al. proposed two correlations for pressure drop and Nusselt number by conducting an experimental study on a square pin fin MCHS [46]. It is important to mention here that, in the literature, correlations of Nusselt number especially are a function of Reynolds number and in some cases Prandtl number too, irrespective of geometry and channel parameters like aspect ratio and spacing. Liu et al. experimentally investigated pin fin MCHS to assess the change in performance under changing pin fin shapes [47].Deionized water was used as the working fluid with a staggered arrangement for pin fins. Elliptical, circular and diamond shapes were considered for analysis. The aforementioned research concluded that the

effect of pin fin shape becomes more dominant at higher mass flow rates. It was found that during relatively low Reynolds number flow, the end wall effects took precedence over fin shapes in determining the Nusselt number. Furthermore, this effect of end wall diminishes as Reynolds number is relatively increased.

Mei et al. focused their research on circular pin fin tip clearance by performing a numerical investigation [48]. It is important to define pin fin tip clearance. Tip clearance is defined as ratio of pin fin height to the height of the channel wall. For example, tip clearance can be varied by taking pin fin height as constant and varying the height of channel wall or vice versa. The aforementioned research opted for the former method. It was found that as pin fin tip clearance was increased, thermal performance diminished while hydraulic performance increased. New correlations for pin fins with tip clearance were also developed in the wake of this research since previous correlations failed to capture the physics of the problem. Peles et al. conducted an experimental study on a circular pin fin MCHS [49]. It was recommended by the authors that for relatively low Reynolds number operation of heat sink, pin fins should have low density while contrary is true for high Reynolds number operation.

Prasher et al. carried out an investigation on crossflow for low aspect ratio and staggered pin fins for square and circle cross sectional shapes, by performing series of experimental tests [50]. Correlations were established for Nusselt number and friction factor as a function of Reynolds number for two ranges of Reynolds number i.e., greater than Reynolds 100 and smaller than Reynolds 100. The research concluded by recommending that more studies on pin fin MCHS must be carried out with an additional purpose of flow visualization. Far et al. used a phase change material as a working fluid on oblique pin fins with different tip clearance, by conducting a numerical investigation [51].It was found that phase change material significantly enhances the thermal performance. This came at the expense of increase in pressure drop which was mitigated by a proposed change in tip clearance. The research concluded that an optimum value of tip clearance existed which provided better heat transfer with phase change material at a relatively low penalty of pressure drop. It is therefore important to realize that an optimum value is desired by researchers in geometric optimization.

Rasouli et al. used a fluorinated fluid PF-5060 as the working fluid and performed experimental tests on eight different heat sinks with diamond pin fins with different aspect ratios and transverse pitch to diameter ratios [52]. The study was carried for low Reynolds number (8 to 1189) laminar flow with an aid of flow visualization. The results were analyzed in the context of vortex shedding. The research concluded with the establishment of new correlations for Nusselt number, accounting for the effects of vortex shedding. Reddy et al. performed a numerical analysis on circular, symmetric airfoil and convex lens shaped pin fin microchannel heat sinks with the purpose of optimization [53]. Important findings included an observation of poor performance of circular pin fins relatively, due to flow separation. The research also focused on removing this flow separation from circular fins using optimization of geometrical parameters but with negative results. Meanwhile convex lens and air foil (symmetric) pin fins were optimized in such a way that their flow separation was reduced to a minimum level.

Geometrical optimization has been a topic of interest for many researchers. The reason for this is because there are infinite number of geometrical modifications one can perform. Generalizing heat transfer problems is a very complex and time-consuming task. Rezaee et al. experimentally and numerically investigated the optimization process of pin fins by their longitudinal pitch and length [54]. It was found that in order to enhance heat transfer, long pin fins should be used near the inlet while near the outlet, fins with less longitudinal pitch should be used. Rozati et al. numerically established that performance of a circular pin fin heat sink is highly dependent on tip clearance [55]. The operating conditions were governed by low Reynolds number flow of the range 5 to 400. It was established that at high Reynolds number flows, tip clearance effects are of minimal importance. Furthermore, it was also found that tip clearance helps mitigate the end wall effects.

Jimenez et al. conducted a numerical investigation to propose unique/novel heat sink design based on changing fin density [56]. The authors carried out their analysis on four different geometrical shapes for pin fins namely, ellipse, circle, flat shape with two rounded sides and square. Of the important findings, one stood out that change in the shape of the pin fin contributes more to the pressure drop

than the heat transfer. It was also found that flat shaped fins with two rounded edges, performed best among all the shapes considered. Jimenez et al. carried out numerical analysis using two configurations of microchannel heat sinks namely offset and in line with changing pin fin density [57]. The research established that the offset configuration thermally outperforms the base case by 1.3 times. Regarding pressure drop it was found that offset case/configuration achieves better thermal performance at the expense of increase in pressure drop.

Shafeie et.al conducted a numerical analysis on pin fin MCHS as well as simple pin fin heat sinks with specific emphasis on the arrangement on pin fins i.e., staggered and oblique configuration [58]. It was found that the heat sink with the highest numerical value of depth along the length of the heat sink performed best, in terms of heat transfer. It was documented that MCHS performed better than its counterpart provided the pressure drop was kept constant.

Singh and Kumar performed a numerical analysis on a pin fin MCHS with an emphasis on the effects produced by changing uniform channel width to non-uniform channel width [59]. It was found that non uniform channel width enhances flow distribution. Because of this reason, Nusselt number was found to be increased by 10% for non-uniform channel width heat sink compared to uniform one. This performance enhancement came at a cost of rise in the pressure drop of 5.7%.

In literature, various working fluids have been used as cooling mediums for pin fin heat sinks. To enhance hydro-thermal performance, researchers have shown considerable interest in testing various working fluids. These working fluids include nano fluids, paraffin slurries, liquid metals, PCM (phase change material) etc.

A great amount of research has been done on the effect of using nano fluids for the enhancement of heat transfer in microchannel heat sinks. In 2005, Chein and Huang proposed a silicon MCHS with nano fluids as coolant [60]. Copper nano particles with volume fractions of 0.3-2% were utilized. Results showed that as Reynolds number and volume fraction are increased, thermal resistance decreases. Lowest thermal resistance value of 0.06 K/W/cm^2 was achieved. Prajapati and Rohatgi conducted an experimental study to observe the effects of heat transfer enhancement by introducing Zinc oxide nano particles in water [61].

It was concluded that heat transfer coefficient 'h' increases by 126% when using zinc oxide nano fluid. Furthermore, pressure drop increases by 23% when the concentration of respective nano particles is increased by 0.1%. Additionally, it was found that surface roughness increases by 137% as the concentration of respective nano particles is increased.

2.1 Novelty of the Design

According to author's best knowledge, the idea of I-shaped pin fins has not been explored previously. This fact attests to the novelty of this design. This design of pin fin is inspired by an I-shape cross section which is employed extensively in structure engineering problems.

This research work is based on the study of effects of geometrical parameters namely pin fin thickness, height and orientation on hydro-thermal performance of a microchannel heat sink. Effects of Reynolds number and heat flux on hydro-thermal performance are also analyzed. Results are established on the basis of various performance parameters.

Chapter 3

Problem Formulation

3.1 Geometrical Modelling

Geometrical modeling is the initial step of problem formulation. Figure 3.1 presents a detailed geometrical description of the microchannel heat sink with I-shaped pin fins. The heat sink has a total length 'L' of 27 mm. It has a width 'W' of 10 mm while having a height 'H' of 3 mm. The two side walls of the heat sink have a thickness 'W_{sw}' of 0.5 mm each. The base of the heat sink 'H_b' has a thickness of 1 mm. Both inlet and outlet of the setup are situated at a distance of 2 mm from the start and end of the pin fins, respectively. The reason for this is to keep the hydraulic diameter same for heat sink, irrespective of the fin shape or dimension. The foot print area of one pin fin is 1 mm^2. It has been kept constant in this study in accordance with the reference study by Bhandari and Prajapati [62], for comparative purposes. It must also be noted that there are 4 rows of pin fins with 12 pin fins in each row, making a total of 48 pin fins. Pin fin thickness is defined by a variable 'X'.

All pin fins are pitched at a distance of 1mm from each other in both directions. Geometric parameters 'H' and 'X' are varied, in the present numerical investigation. Parameter 'H' varies from 0.75 to 2 mm with an increment of 0.25 mm. Parameter 'X' varies from 0.1 to 0.4 mm with an increment of 0.1 mm. Table 3.1 tabulates fin height and fin thickness value ranges.

Water is taken as the working fluid with its thermophysical properties as a function of absolute temperature. Copper is used as the material for the heat sink since copper has one of the highest thermal conductivities among metals and alloys. At a maximum fin height of 2 mm, the heat sink will become fully closed while at fin heights less than 2 mm, it will be considered as an open heat sink. Open and closed heat sink configurations differ on the basis of the flow of working fluid. In a closed configuration, only channel passages are present for the working fluid to flow while in the open configuration, top space unoccupied by the pin fins is also present for the working fluid thus fully submerging the pin fins.

Three-dimensional geometries are created in PTC CREO 4.0 CAD software. Surface area of each geometry is calculated within the CAD software. Surface area is of prime importance in conjugate heat transfer problems and plays a vital role in post processing. A heat sink geometry without pin fins is also created, as mentioned in the reference paper. This heat sink geometry is needed to normalize temperature and pressure derived results in to thermal performance factor, ψ.

Table 3.1: Geometrical parameters

Variable	Value
Dimension of pin fin footprint	1 mm^2
Pin fin height (H)	0.75-2 mm
Thickness of pin fin (X)	0.1-0.4 mm

3.2 Solution Methodology

For computational modelling, commercial computational tool Ansys Fluent 2021 R2 is used. Heat sink geometries created in the CAD software are directly imported in the computational software. As mentioned before, the physical problem is a conjugate three-dimensional (3D) heat transfer problem with constant heat flux applied at the bottom wall. Conduction and convection take place simultaneously. Furthermore, the solution model is time independent (steady state).

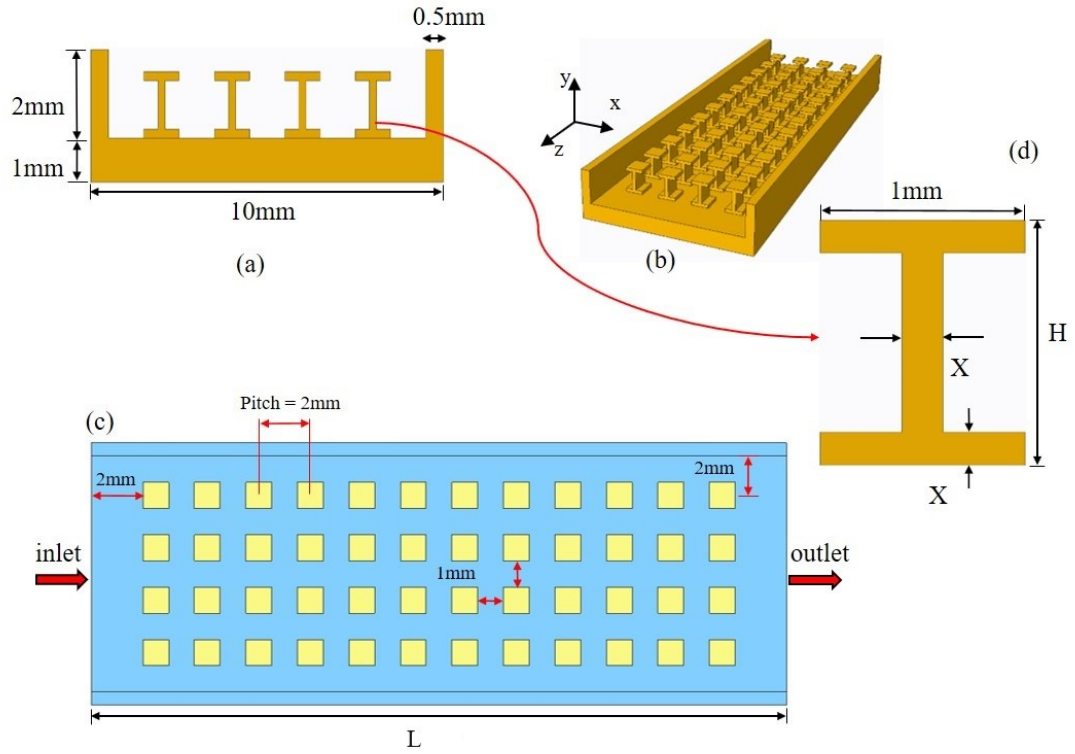

FIGURE 3.1: Geometry of the heat sink (a) cross sectional view (b) isometric view (c) top view (d) cross section of a single I-shaped pin fin

Reasonable assumptions are equally important to simplify the computational problem. Following are the assumptions,

• Outer walls are adiabatic / completely insulated-adiabatic boundary condition on outer walls is necessary to accurately account for heat dissipation only from the bottom wall.

• No slip condition at the wall surface-without no slip condition, boundary layer is not formed on the heat sink surface.

• Incompressible fluid-water is an incompressible fluid irrespective of the flow velocity.

• Natural convection is negligible-Only heat transfer due to forced convection is analyzed.

• Heat transfer due to radiation is negligible.

• Time independent laminar flow-steady state is considered because flow parameters are not a function of time.

• Copper-thermophysical properties are independent of absolute temperature.

3.2.1 Governing Equations

Continuity, momentum and energy equations are the three main equations which are used to model this computational problem. Following are the three equations,

$$\nabla \cdot (\rho \overrightarrow{V}) = 0 \tag{3.1}$$

$$\nabla \cdot (\rho \overrightarrow{V} \cdot \nabla \overrightarrow{V}) = -\nabla p + \mu \nabla^2 (\overrightarrow{V}) + \rho \overrightarrow{g} \tag{3.2}$$

$$\nabla \cdot (\rho c_p (\overrightarrow{V} \nabla T)) = \nabla \cdot (k \nabla T) \tag{3.3}$$

Where ρ is the density of the fluid in kg/m^3,$\overrightarrow{V}$is the velocity vector of the fluid at motion in m/s. T is the temperature in K, k is the thermal conductivity (for both solid and liquid) in $W/(m.K)$. Moreover p and μ are the pressure and dynamic viscosity of the fluid in Pa and Pa.s respectively. Furthermore c_p is the coefficient of heat capacity at constant pressure in $kJ/(kg.K)$.

3.2.2 Fluid Properties

Thermophysical properties of liquid water are a function of temperature, 'T'. It is thus important to implement these properties as a function of absolute temperature in the computational model. This is achieved by using the polynomial functions in the computational software. These correlations are referenced from [63] and they are valid in the range of 278-368 K, at atmospheric pressure. Following are the correlations,

$$\rho(T) = 765.33 + 1.8142T - 0.0035T^2 \tag{3.4}$$

$$c_p(T) = 28070 - 281.7T + 1.25T^2 - (2.48 \times 10^{-3})T^3 + (1.857 \times 10^{-6})T^4 \tag{3.5}$$

$$k(T) = -0.5752 + (6.397 \times 10^{-3})T - (8.151 \times 10^{-6})T^2 \tag{3.6}$$

$$\mu(T) = (9.67 \times 10^{-2}) - (8.207 \times 10^{-4})T + ((2.344 \times 10^{-6})T^2 - (2.244 \times 10^{-9})T^3 \tag{3.7}$$

3.2.3 Boundary Conditions

The inlet of the heat sink is given a velocity inlet boundary condition with a uniform profile. A constant temperature value of 300 K is also provided, at the inlet. Outlet is set as a pressure outlet boundary condition. The bottom wall is provided with a uniform heat flux of constant value. Heat is conducted in the normal direction(y) through a bottom wall thickness of 1 mm. Heat flux values vary from 75 to 150 kW/m^2. All the walls except the bottom wall are insulated i.e adiabatic boundary condition. Reynolds number ranges from 200 to 800. Reynolds number is a non dimensional parameter which is a ratio of inertial effects to viscous effects of a fluid in motion. It's formula is shown below. Inlet velocities are calculated based on the respective Reynolds number. For Reynolds number of 200-800, the corresponding flow velocities are 0.05 m/s, 0.10 m/s, 0.16 m/s and 0.21 m/s respectively. Figure 3.2 presents the schematic diagram of boundary conditions applied on the geometrical model.

$$Re = \frac{\rho V_{in} D_h}{\mu} \tag{3.8}$$

Where D_h is the hydraulic diameter in mm while V_{in} is the inlet velocity in m/s.

3.2.4 Numerical Methods

Owing to the relatively low value of maximum Reynolds number, the flow is considered as laminar. SIMPLE algorithm is employed for pressure-velocity coupling, which was first proposed by Patankar[64]. Second Order Upwind schemes are used to discretize energy and momentum equations. Second order discretization

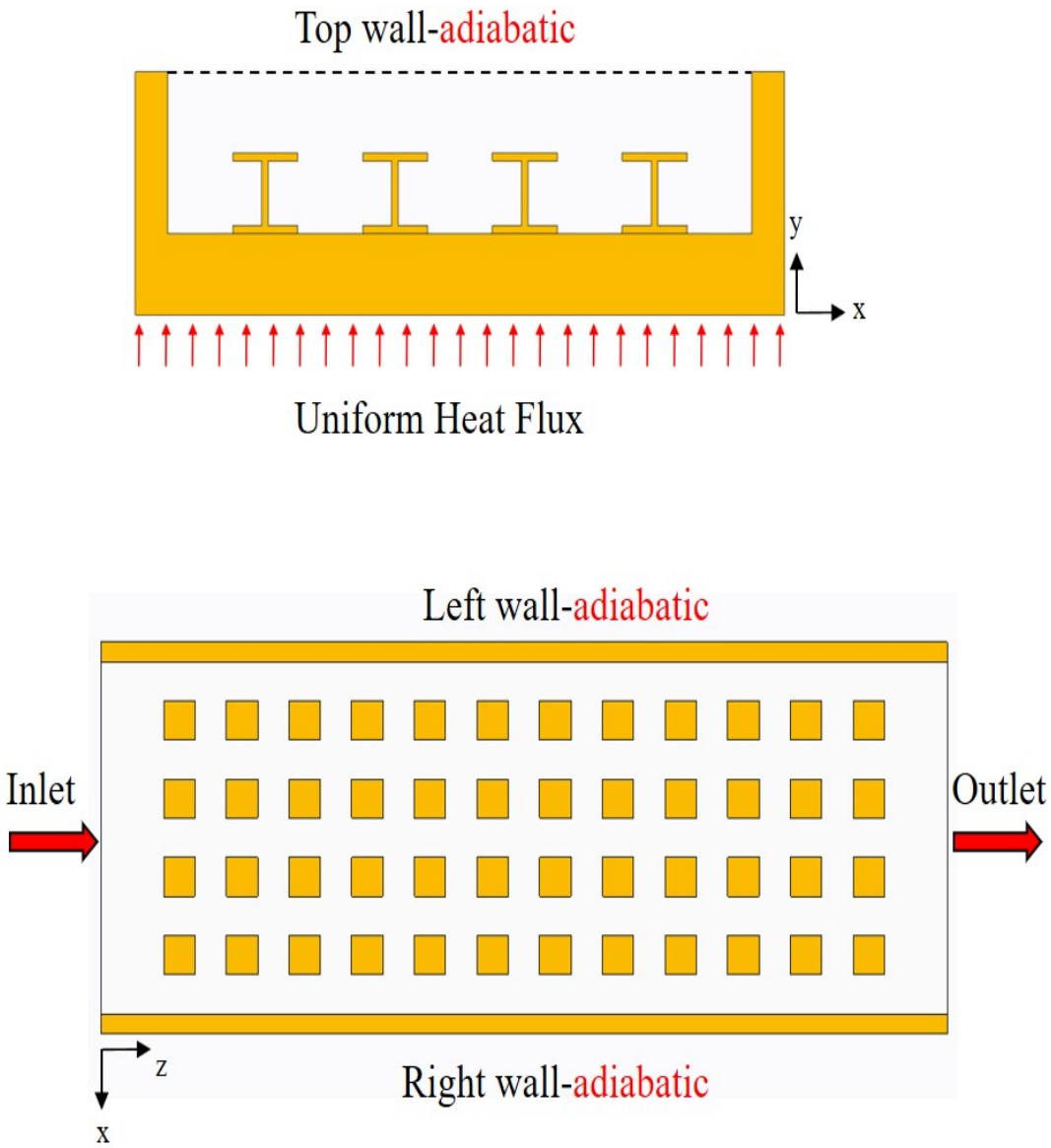

FIGURE 3.2: Schematic diagram representing boundary conditions on the geometry

schemes provide greater solution accuracy than first order schemes. First Order Upwind schemes are the simplest and most basic form of discretization. In this context, only second order upwind schemes are used. For cases involving pin fins at certain orientations, COUPLED algorithm is used. This is because cases with pin fin orientation converged only using COUPLED algorithm. Energy equation, x, y and z components of the velocity are set to a residual of 10^{-6}. Whereas continuity equation is set to 10^{-5}. Continuity equation is set to 10^{-5} becase difference between 10^{-5} and 10^{-6} values is negligible. Furthermore the time required to reach 10^{-6} continuity equation residual is much significant compared to 10^{-5} residual.

3.2.5 Grid Generation and Grid Independence

A high-quality mesh is needed to accurately predict the computational results. Hexahedral elements are created on the heat sink by slicing the heat sink and flow domain in several blocks/parts. This method of slicing is carried out in Ansys Fluent meshing domain.

A mesh independence analysis is equally important to validate the numerical model. In order to achieve mesh independence, six different meshes were considered based on their element size. Mesh independence study is carried out for an I-shaped pin fin heat sink geometry with fin height 'H' of 1 mm, thickness 'X' of 0.1 mm. Table 3.2 summarizes element size and number of elements for coarse, medium and fine mesh categories.

TABLE 3.2: Mesh types based on element size

No	Mesh Category	Number of Elements	Element Size (m)
1	Coarse-1	1×10^{5}	8×10^{-5}
2	Coarse-2	3×10^{5}	6×10^{-5}
3	Coarse-3	7×10^{5}	5×10^{-5}
4	Medium-1	1.1×10^{6}	4×10^{-5}
5	Medium-2	1.6×10^{6}	3×10^{-5}
6	Fine	3.7×10^{6}	1.8×10^{-5}

Figure 3.3 presents mesh with 1.6 million mesh elements with different views, (a) isometric view, (b) cross sectional view and (c) individual pin fin cross-section. For this mesh, Element size chosen for pin fins is 3×10^{-5} m. As shown in Figure 3.3(c), with this element size, a total number of three mesh elements are formed on a thickness of 0.1 mm.

For accurate results, it is important to have a minimum number of 3 mesh elements on thickness of 0.1 mm. The reason being that, for a small thickness of 100 μm, 3

mesh elements each of approximately 33 μm thickness provide an optimum mesh setting, keeping in view the constraints on computational resources. Furthermore it is important to note that mesh density on pin fins must be higher than mesh density on heat sink and flow domain. This is because pin fins are extended surfaces and act as the primary contributor towards heat transfer.

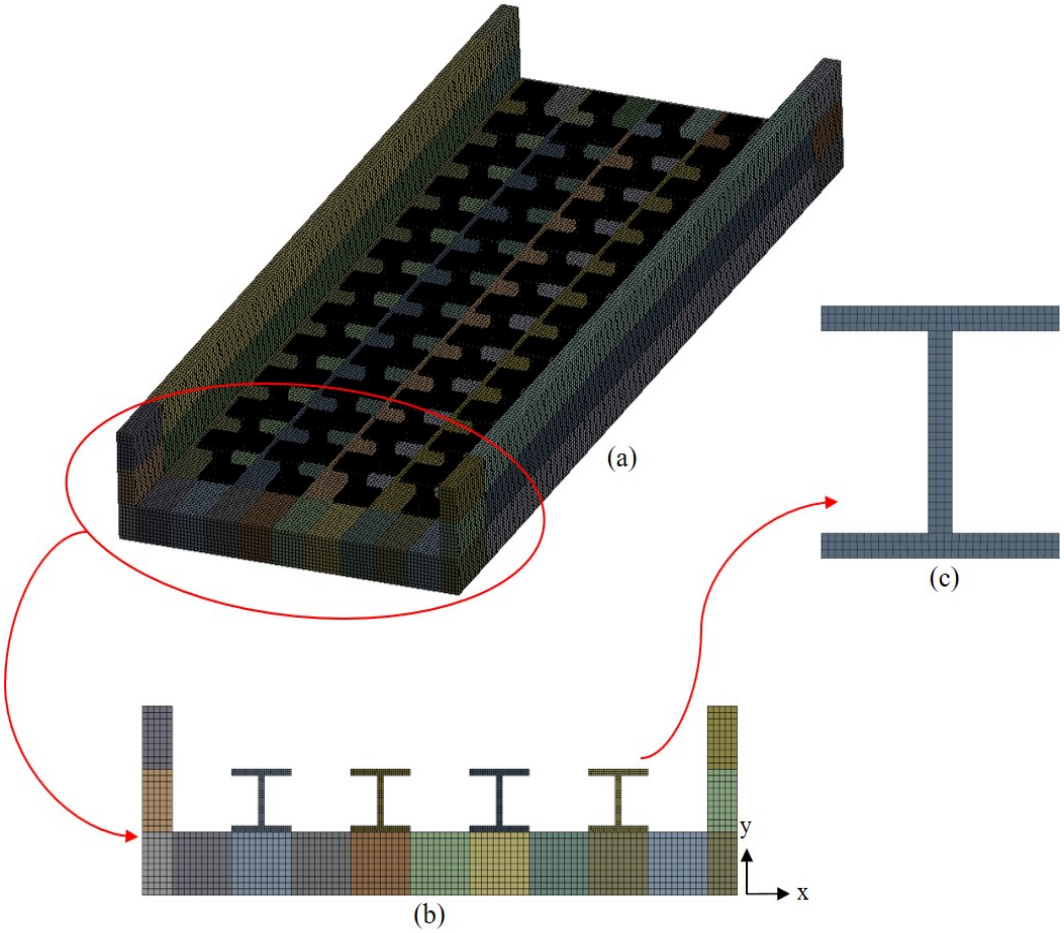

FIGURE 3.3: Mesh (a) isometric view, (b) cross-sectional view, (c) pin fin cross-section

Figure 3.4 shows plot for grid independence analysis. Pressure drop, ΔP is plotted against number of elements. For the grid independence analysis, simulations are carried out at the heat flux value and Reynolds number of 150 kW/m^2 and 800 respectively. Number of elements indicate type of mesh i.e coarse, medium or fine. Minimum number of elements are 1×10^5 while maximum number is 3.7×10^6. Trend of pressure drop, ΔP tends to form a constant horizontal line after 1.1×10^6 number of elements. Mesh with 1.6×10^6 elements is chosen for simulations of all the cases. The is because the difference in pressure drop value is less than 1% when compared with fine mesh having 3.7×10^6 elements.

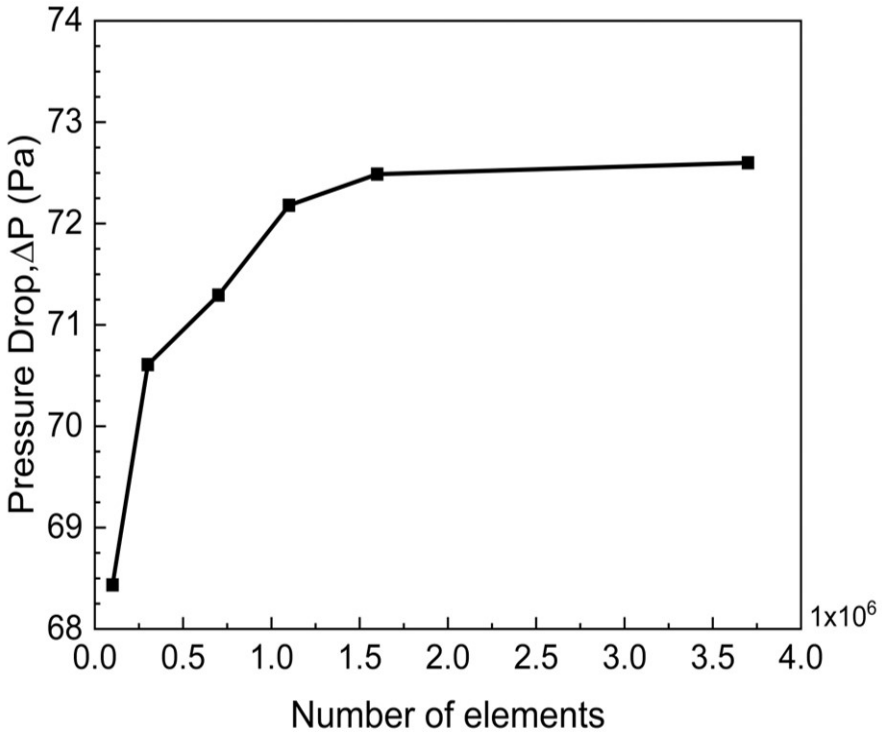

FIGURE 3.4: Grid independence based on pressure drop, ΔP

3.2.6 Performance Parameters

Base temperature and pressure drop are two fundamental output parameters of these numerical simulations. Base temperature is calculated as area weighted average of temperature at the bottom wall where heat flux is applied. Whereas pressure drop is calculated as the difference of area weighted average of pressure at inlet and outlet, respectively. Base temperature directly corresponds to the thermal effectiveness of the heat sink. A lower base temperature value indicates better heat transfer. On the other hand, a lower value of pressure drop indicates better hydraulic performance. Pressure drop value is dependent on the degree of obstructions that the flow encounters. In this retrospect, a heat sink with no pin fins has the lowest possible value of pressure drop. This of course comes at the cost of thermal performance. A heat sink with no pin fins has the worst thermal performance.

Nusselt number (average) and thermal performance factor, denoted as $\overline{Nu}$ and ψ respectively, are derived quantities. As mentioned in previous chapter, Nusselt number is dependent on variable parameters namely contact surface area, average temperature of contact surface area and bulk temperature (average temperature

of flow domain). On the other hand, ψ is derived from a mathematical relation based on pressure and Nusselt number values of heat sink with pin fins and heat sink without pin fins. Furthermore ψ incorporates both thermal and hydraulic performance. A ψ value of more than 1 indicates enhancement in the heat sink performance.

Nusselt number, '$\overline{Nu}$' is calculated from average heat transfer coefficient. Average heat transfer coefficient is a function of three parameters namely, effective heat flux, fin base temperature, T_b and bulk temperature, T_{bulk} of the flow domain. Bulk temperature is extracted from Ansys Fluent by describing a temperature variable for volume weighted average of flow domain.

Where q_{eff} is a function of area ratio. Following is the formula for q_{eff},

$$q_{eff} = q \times \frac{A_{bw}}{A_{csa}} \tag{3.9}$$

Where A_{bw} is the bottom wall surface area. Furthermore A_{csa} is the contact surface area between solid and liquid medium. It includes pin fin area as well as inner walls (left, right and bottom) area. Here it is important to mention that A_{csa} is a variable parameter dependent on fin height and fin aspect ratio (geometrical features). Moreover, it is also crucial to note that A_{bw} remains constant for all cases and it has a value of 270 mm^2 . At a fin height of 1 mm, square pin fins have a solid liquid contact surface area A_{csa} of 543 mm^2. Contact surface area plays an important role in heat transfer analysis. For instance, an I-shaped pin heat sink having fin height, 'H' of 1 mm and thickness, 'X' of 0.2 mm has A_{csa} of 573.72 mm^2. It is therefore important to realize that change in surface area significantly effects the magnitude of heat transfer in a heat sink .

$$D_h = \frac{4A_c}{p} \tag{3.10}$$

$$\overline{h} = \frac{q_{eff}}{T_{avg,cw} - T_{bulk}} \tag{3.11}$$

$$\overline{Nu} = \frac{\overline{h}D_h}{k} \tag{3.12}$$

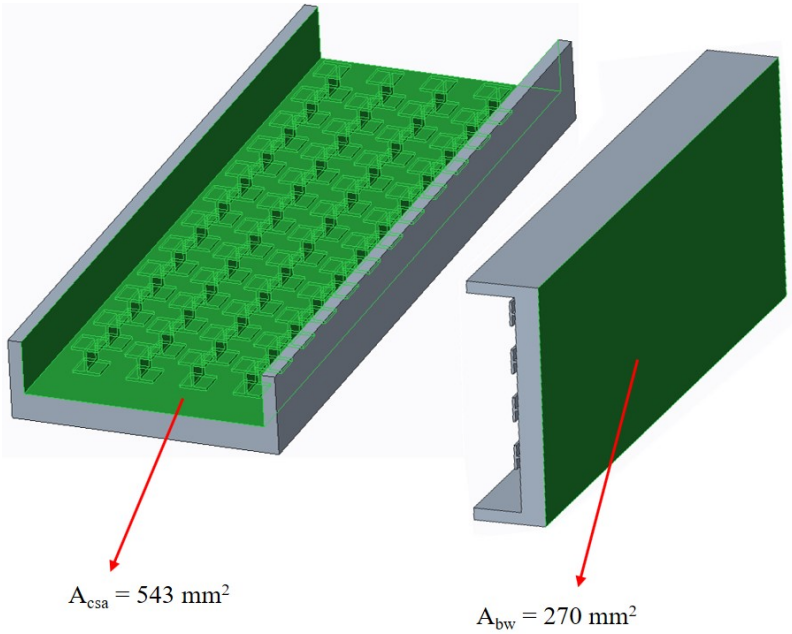

FIGURE 3.5: Representation of A_{csa} and A_{bw}

$$\psi = \frac{\overline{Nu}/\overline{Nu}_o}{\sqrt[3]{(\Delta P/\Delta P_o)}} \tag{3.13}$$

Formulas for hydraulic diameter 'D_h', Nusselt number '$\overline{Nu}$', ψ and convective heat transfer coefficient 'h' are described above. It is worth mentioning that variable 'k' in the Nusselt number formula represents thermal conductivity of the working fluid at bulk or film temperature. In the formula of heat transfer coefficient 'h', $T_{avg,cw}$ corresponds to the temperature of solid-liquid contact surface area, within the heat sink. Furthermore D_h is the hydraulic diameter of the heat sink. Hydraulic diameter is D_h is defined as 4 times the cross-sectional area of the heat sink divided by its perimeter. Throughout this numerical study, hydraulic diameter remains constant i.e 3.27 mm, irrespective of fin shape and size.

3.2.7 Validation Study

It is important to validate the numerical model with the existing literature. Model validation has been carried out with existing numerical study on square pin fin microchannel heat sink with fin height of 1 mm and constant heat flux value of 150 kW/m^2. Figure 3.6 presents plots of base temperature, T_b and pressure drop, ΔP. For the temperature graph, a maximum error of 1.28% is encountered at a

Reynolds number of 800. For the pressure graph, a maximum error of 1.34% is also encountered at a Reynolds number of 800. It is worth mentioning here that as Reynolds number increase, the level and intensity of flow disturbance also increase leading to more complex solution model. By carrying out a comparison of pressure drop and fin base temperature, it can be said that the maximum percentage error of any parameter at any instant is less than 5%. Thus, providing a validating argument to further this research.

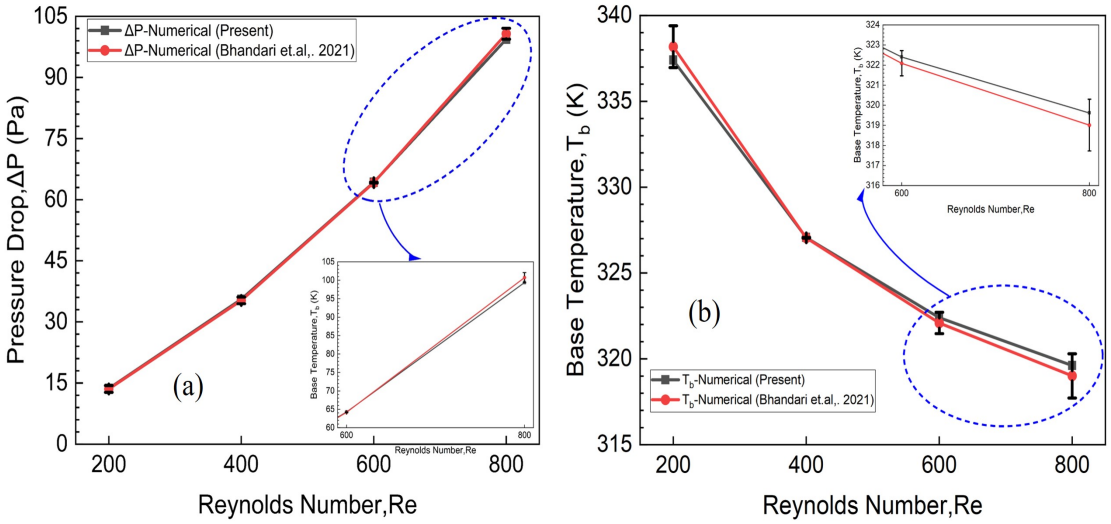

FIGURE 3.6: Validation study (a) base temperature vs Reynolds number (b) pressure drop vs Reynolds number

Chapter 4

Effects of Fin Height and Thickness on Hydro-Thermal Performance

This chapter comprehensively documents the results derived from the numerical simulations. Multiple line plots and contours are created form the data extracted from numerical simulations. In addition, qualitative reasonings are presented in support of the quantitative results. Furthermore, the importance of pin fin surface area and its effects on performance parameters is established. Streamline plots are also created in this context of qualitative reasonings. Simulations have been carried out at Reynolds number of 800 and heat flux of 150 kW/m^2. Highest value of Reynolds number and heat flux are chose for initial simulations because at these values, the heat sink gives the highest values of performance parameters. An optimum case is identified from these simulations, based on thermal performance factor, ψ.

For the optimum case, simulations have been carried out for whole range of Reynolds number and heat flux values. Table 4.1 presented below summarizes these simulations. Based on the values of ψ and $\overline{Nu}$, L=1.5 mm and X=0.4 mm case is considered as optimum. A total number of 64 cases have been simulated for the optimum case based on the parameters in the table.

TABLE 4.1: Simulated cases

No	Cases	Re	Heat flux (kW/m^2)
1	L=1.5 mm, X=0.1 mm	200	75
2	L=1.5 mm, X=0.2 mm	400	100
3	L=1.5 mm, X=0.3 mm	600	125
4	L=1.5 mm, X=0.4 mm	800	150

4.1 Surface Area and Cross-sectional Shape Sizes of Pin Fins

Figure 4.1 presents cross sections of I-shaped pin fins based on varying values of fin height 'H' and thickness 'X'. Numerical values of surface area are also presented along with each pin fin cross section. This figure is a representation of the effects of change on a pin fin cross section due to varying fin height 'H' and fin thickness 'X'. In forced convection problems, solid-liquid contact surface area is of principal importance. It is an important design parameter which is frequently optimized by researchers. In this context, pin fin cross section plays an important role in determination of performance of the heat sink. For the most part, pin fin cross section determines the flow behavior within a heat sink. Each pin pin cross section presented in the figure below exhibits a distinct flow behavior. This flow behavior has a profound impact on hydro-thermal performance of MCHS. Smallest surface area value of 4.81 mm^2 exists for H=0.75 mm and X=0.1 mm. Furthermore, highest surface area value of 8.76 mm^2 exists for H=2 mm and X=0.4 mm.

The importance of surface area cannot be underestimated. Convection heat transfer is dependent only on three parameters namely heat transfer coefficient, surface area and temperature difference. Heat transfer coefficient is itself dependent upon Reynolds number and thermophysical properties of the working fluid.

H (mm) \ X (mm)	0.1	0.2	0.3	0.4
0.75	4.81 mm²	5.04 mm²	5.19 mm²	-
1	5.36 mm²	5.64 mm²	5.84 mm²	5.96 mm²
1.25	5.91 mm²	6.24 mm²	6.49 mm²	6.66 mm²
1.5	6.46 mm²	6.84 mm²	7.14 mm²	7.36 mm²
1.75	7.01 mm²	7.44 mm²	7.79 mm²	8.06 mm²
2	7.56 mm²	8.04 mm²	8.44 mm²	8.76 mm²

FIGURE 4.1: Surface area and cross-sectional shape sizes of pin fins

On the other hand, Surface area is an independent parameter which is not influenced by any outside parameter. Both surface area and heat transfer coefficient influence the temperature difference which in turn effects the heat transfer. Effect of surface area on hydro-thermal performance is thus an important aspect of this study.

4.2 Performance Parameters v/s Thickness for Different Fin Heights H

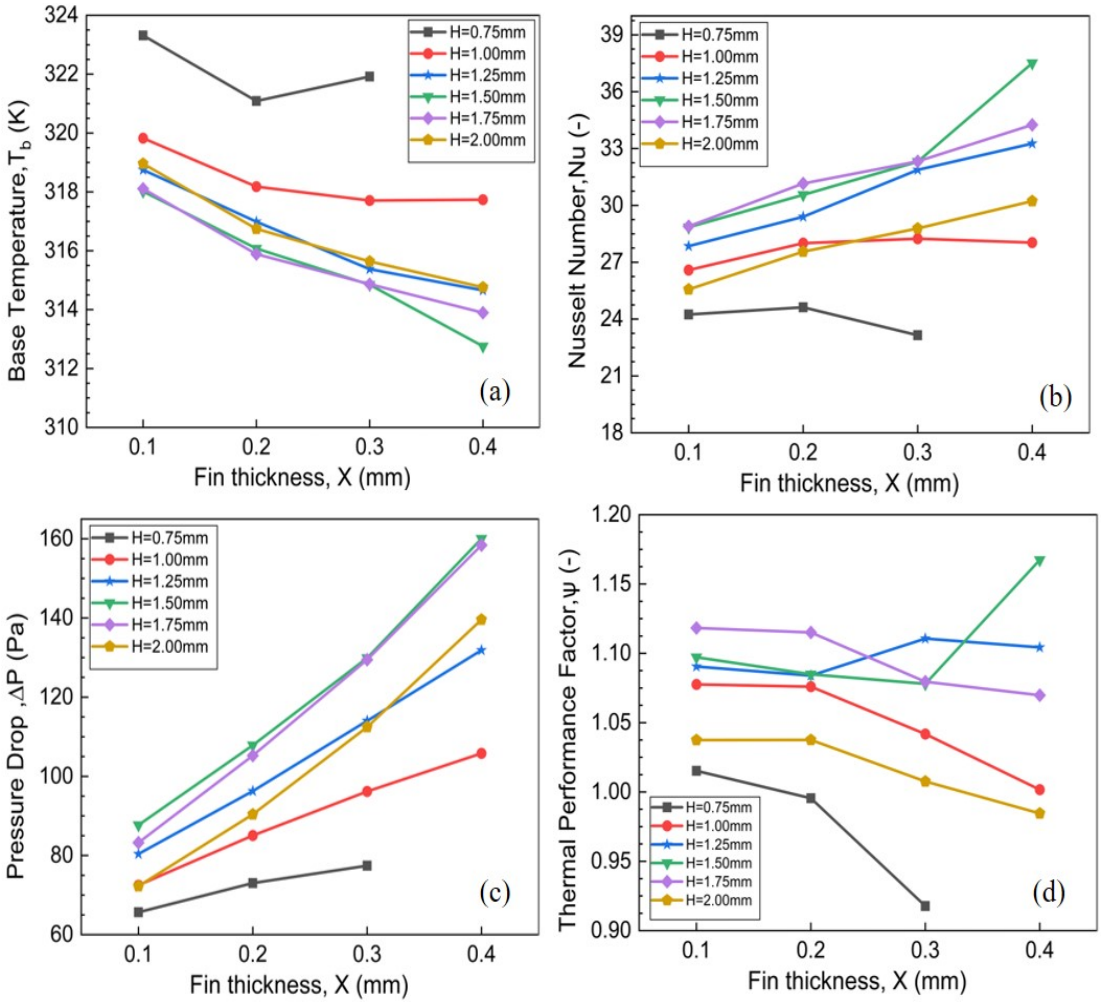

FIGURE 4.2: (a) Base temperature, (b) Nusselt number, (c) pressure drop, (d) TPF against varying fin thickness for all the fin heights

Figure 4.2 presents plots of performance parameters against fin thickness 'X' for varying fin heights 'H', at Reynolds number of 800 and heat flux value of 150 kW/m^2. Fin thickness 'X' varies from 0.1-0.4 mm while fin height 'H' varies from 0.75-2 mm.

Base temperature, T_b is the fundamental performance parameter. It is an indicator of thermal performance of a microchannel heat sink. A lower value of base temperature is desired. In Figure 4.2 (a) the values of base temperature, T_b decrease as thickness is increased, for all the cases except fin height of 0.75 mm and 1 mm. The highest value of base temperature is 323.3 K for H=0.75 mm and X=0.1

mm while the lowest value is 312.7 K for H=1.5 mm and X=0.4 mm. Increasing fin height to the maximum limit does not decrease T_b linearly, instead T_b starts to increase after a certain value of H. This is evident by the lowest value of T_b (312.7 K) for fin height of 1.5 mm. Nusselt number, $\overline{Nu}$ is an important non dimensional performance parameter which correlates convection and conduction in a conjugate heat transfer problem. A higher value of Nusselt number is desired. Effects of base temperature T_b are directly translated to Figure 4.2 (b) presenting the values of Nusselt number. Figure 4.2 (b) shows that the value of Nusselt number increases with increasing fin thickness for all the cases except fin heights of 0.75 mm and 1 mm. The highest value of Nusselt number is 37.5 for H=1.5 mm and X=0.4 mm while the lowest value is 23.1 for H=0.75 mm and X=0.3 mm.

In the design of a microchannel heat sink, pumping power is an aspect of principal importance. A higher value of pumping power negatively affects the costs of operating a heat sink. Line plots of pressure drop presented in Figure 4.2 (c) shows that for a constant fin height, pressure drop increases with increasing fin thickness. The value of pressure drop also increases with increasing fin heights, except for the fin height of 2 mm. Moreover, pressure drop values for fin height of 1.5 mm and 1.75 mm are comparable. It is important to note here that a fin height of 2 mm depicts a completely closed heat sink, unlike previous fin heights where heat sink is open. The highest value of pressure drop is 160.0 Pa for H=1.5 mm and X=0.4 mm while the lowest is 65.6 Pa for H=0.75 mm and X=0.1 mm.

Thermal performance factor, ψ is an important parameter, representing hydrothermal performance. It incorporates all the important parameters and presents a comprehensive picture of the performance. A higher value of ψ is desired for optimal performance. In Figure 4.2 (d), thermal performance factor is presented which encapsulates all the performance parameters discussed beforehand, namely base temperature, Nusselt number and pressure drop. For a constant fin height, value of ψ decreases with increasing fin thickness, except fin heights of 1.25 mm and 1.5 mm. The highest value of ψ is 1.16 for H=1.5 mm and X=0.4 mm while the lowest value is 0.91 for H=0.75 mm and X=0.3 mm. A ψ value of 1.16 represents performance enhancement of 13.8% over the benchmark case(ψ=1). Contact surface area has a direct impact on all the performance parameters. For context,

contact surface area of case H=1.5 mm, X=0.4 mm and case H=0.75 mm, X=0.3 mm is 656.2 mm^2 and 552.1 mm^2 respectively, constituting a difference of 15.8%.

4.3 Velocity Contours at X=0.4 mm for Varying Fin Heights

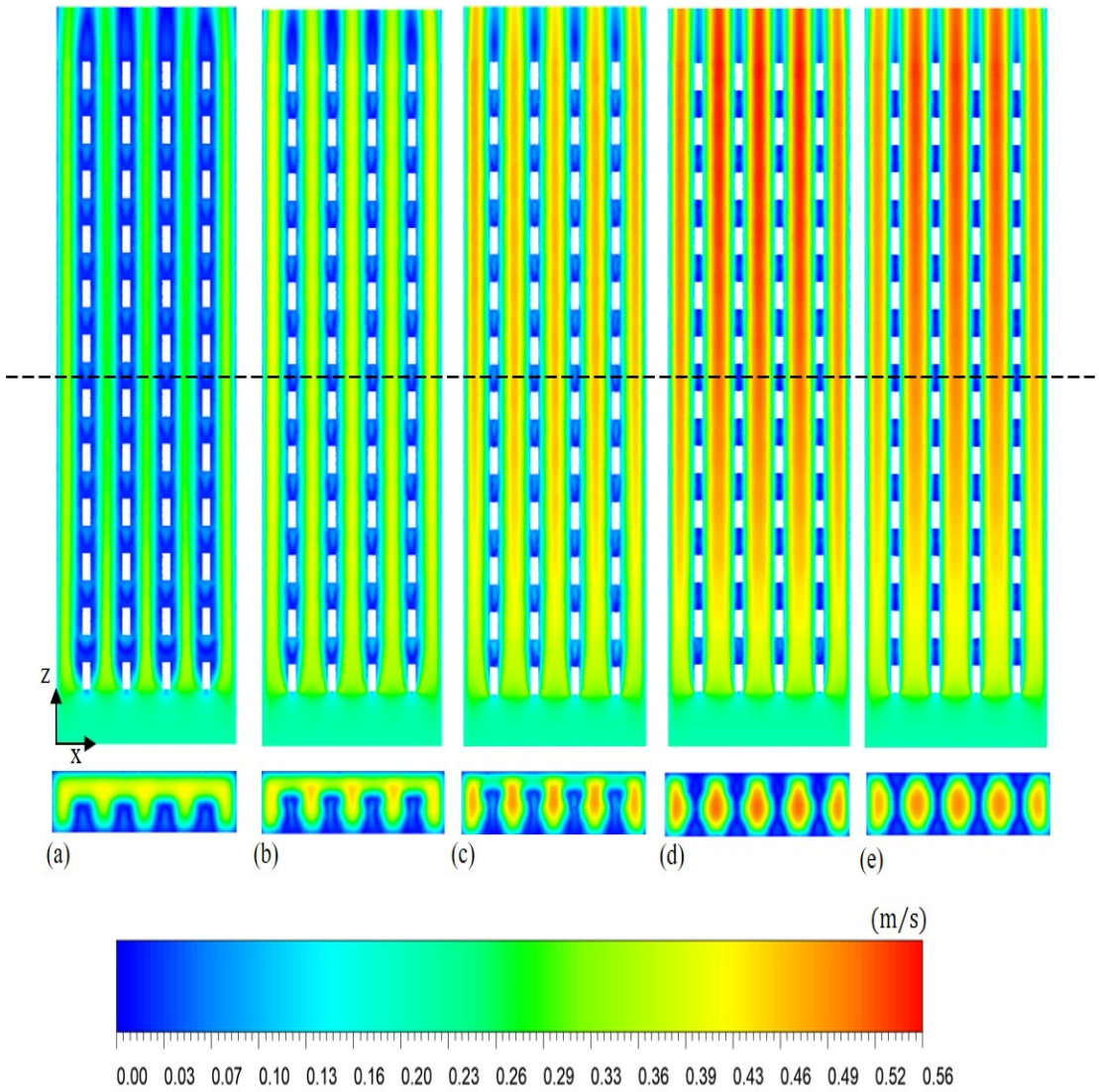

FIGURE 4.3: Velocity contours at X=0.4 mm for varying fin heights

In order to investigate the trends of performance parameters presented in Figure 4.2, contours plots of the important properties need to be investigated.Figure 4.3 presents velocity contours at mid-fin (zx plane) and at z=13.5 mm (xy plane) for fin heights of (a) 1 mm, (b) 1.25 mm, (c) 1.5 mm, (d) 1.75 mm and (e) 2 mm for a constant fin thickness of 0.4 mm. Reynolds number is 800 while heat flux is 150

kW/m^2. Velocity profile has a direct profound impact on temperature profiles in a microchannel heat sink.

Figure 4.3 (a) (mid-fin contour), depicting 1 mm fin height, has a maximum velocity magnitude of 0.35 m/s. This is the lowest value of velocity among all fin heights. In the context of quantification of velocity magnitude, flow regions with highest velocity exist in the channels present between the fin columns. Flow present in the channels accelerate downstream as it moves past the first row of pin fins. The peak velocity magnitude values emerge at a certain distance from the inlet. This flow pattern is also common among all fin heights. Furthermore, channels adjacent to the heat sink wall depict comparatively lower values of velocity. This is due to effects of the sidewall on the velocity profile. Figure 4.3 (d) (mid-fin contour), depicting 1.75 mm fin height, has a maximum velocity value of 0.55 m/s. This is the highest value of velocity among all fin heights. The difference between the limiting values of 0.35 m/s and 0.55 m/s is 36.3%. Generally, it is true that higher the velocity, higher the value of convective heat transfer coefficient will be. Yet despite all this, the lowest base temperature exists for fin height of 1.5 mm. The reason for this lies in the fact that, as fin height increases, temperature at the top portion of the fin reduces substantially compared to the temperature at the base of the fin, due to slow heat conduction. Thus, temperature gradient between flow and surface at the top portion of the pin fin becomes very low. Figure 4.3 (c) (mid-fin contour), representing 1.5 mm fin height, has a maximum velocity value of 0.49 m/s. Comparing with fin height of 1.75 mm, a difference of 10.9% is recorded. There exist regions of recirculation behind the pin fins where velocity magnitude is zero. These recirculation regions are formed as velocity streamlines reverse their direction turning in to that specific region.

Velocity contours at z=13.5 mm form the inlet (xy plane) present a cross sectional view of the flow physics. Each fin height has its unique and distinct contour. Regions of maximum velocity are present at a certain distance, from pin fin cross sections. In the context of heat transfer, fluid flow from top surface of the pin fins has crucial importance. As fin height increases, size of the passage ways for fluid flow decreases. At a fin height of 2 mm, heat sink is completely closed thus working fluid is rendered incapable of transferring heat from the top surfaces of pin

fins. In this regard, contribution of solid-fluid contact surface area to heat transfer is decreased, for a closed heat sink. Solid-fluid contact surface area bears a critical importance. Above the pin fins, fin height of 1.5 mm has a free passage volume of 121.5 mm^3 (0.5 mm×9 mm×27 mm). On the other hand, fin height of 1.75 mm has a free passage volume of 60.75 mm^3 (0.25 mm×9 mm×27 mm). This corresponds to a difference of 50%. Compared to fin height of 1.75 mm, 50% increase in top passage volume for H=1.5 mm, contributes in better heat transfer and reduction in base temperature. An optimum fin height provides enough clearance for the fluid to transfer heat from the top of pin fins.

4.4 Temperature Contours:X=0.4 mm for Varying Fin Heights

Temperature profiles provide an in-depth view of the effects of heat transfer via extended surfaces. Temperature profile shows the development of thermal boundary layer and the regions of lower and higher temperature. Figure 4.4 shows temperature contours at mid-fin (z-x plane) and at z=13.5 mm (xy plane) for fin heights of (a) 1 mm, (b) 1.25 mm, (c) 1.5 mm, (d) 1.75 mm and (e) 2 mm for a constant fin thickness of 0.4 mm. Reynolds number is 800 while heat flux is 150 kW/m^2. Figure 4.4 (a) (mid-fin contour), represents fin height of 1 mm having the highest temperature of 320.4 K. On the contrary, fin height of 1.5 mm depicted by Figure 4.4 (c) (mid-fin contour), has the lowest temperature of 314.3 K. Temperature profile is dependent on the behavior of velocity profile in a forced convection heat transfer problem. Thus, for the most part, velocity profile dictates the temperature profile. For the fin height of 1 mm, it is observed that relatively low temperature values exist right behind the first row of pin fins. A close observation of Figure 13 (a) (mid-fin velocity contour) reveals the presence of the initial wake formation around and behind the first row of pin fins. Flow recirculation/flow mixing gives rise to enhanced heat transfer. As flow moves downstream, its temperature increases due to the temperature gradient between the fluid and fin surfaces. Moving further downstream we see higher temperature values. Since fluid temperature

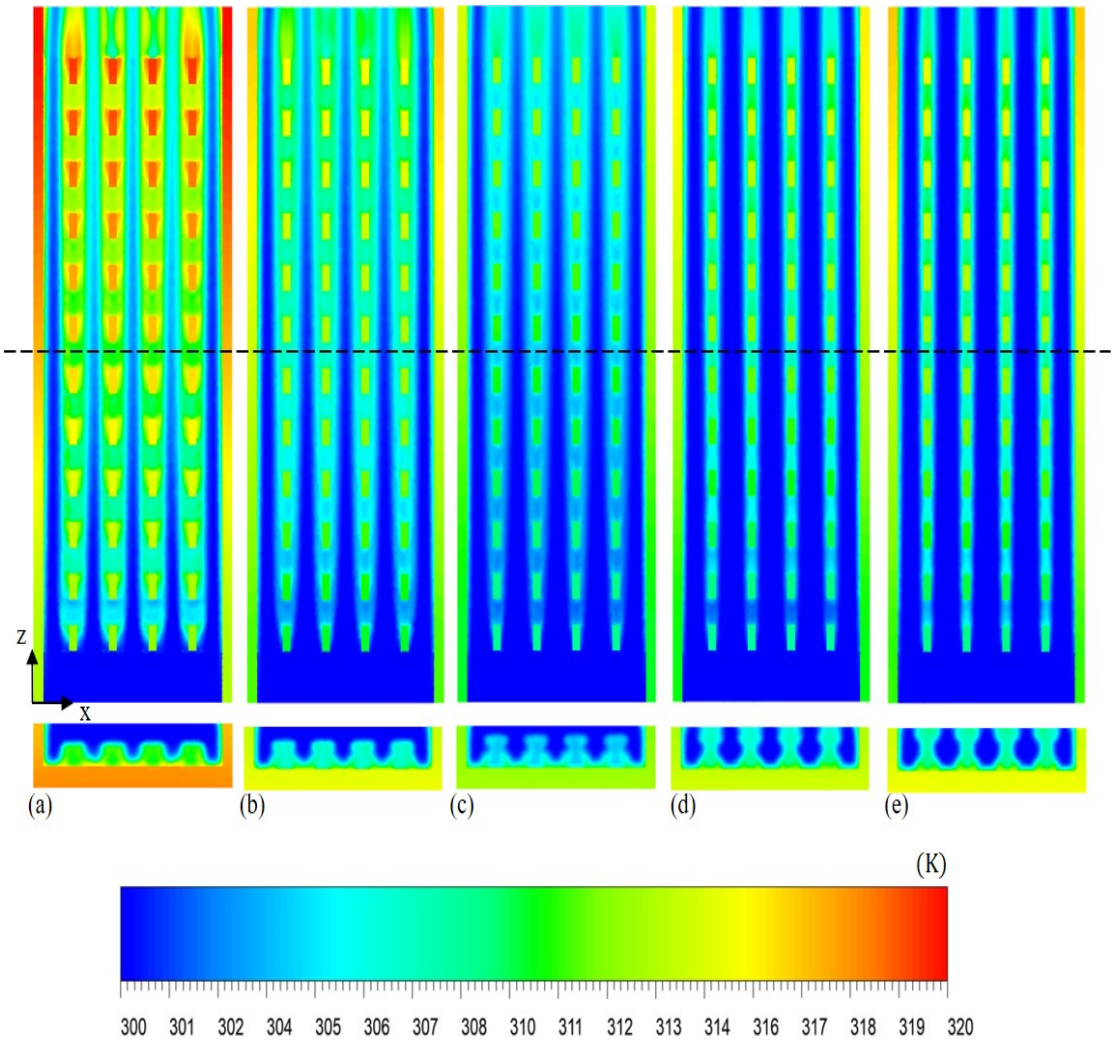

FIGURE 4.4: Temperature contours at X=0.4 mm for varying fin heights

increases as it flows, at the last part of heat sink, the temperature difference is substantially low to provide effective heat transfer. This is evident by higher temperatures present at the fins in the last part of heat sink. Figure 4.4 (c) (mid-fin contour) has the lowest temperature values. For a fin height to have lowest temperature values, it must have sufficient height for maximum heat transfer as well as sufficient top clearance i.e distance from top of the pin fin to the top wall. As mentioned before, compared to H=1.75 mm, H=1.5 mm has 50% more free passage volume at the top of pin fins. According to Bhandari and Prajapati, availability of less open space on top of pin fins for H=1.75 mm has unfavorable effects on heat transfer when compared with H=1.5 mm [62].Due to relative unavailability of open space, H=1.75 mm shares flow characteristics of completely closed heat sink i.e H=2 mm. In this regard, fin height of 1.5 mm depicts better flow induced thermal characteristics and acts as an optimum fin height.

Temperature contours at z=13.5 mm form the inlet (xy plane) are required to complement the discussion of temperature profiles. From Figure 4.4 (a) till Figure 4.4 (e), cross sectional views of the temperature profile are presented. At the bottom wall cross section, highest temperature values are observed for Figure 4.4 (a), while lowest values are observed for Figure 4.4 (c). A close inspection reveals that lowest part of the pin fin cross-section where it connects with base of heat sink, has the highest temperature. This observation is common for all fin heights. Moving up the pin fin cross section, low temperature values are observed, indicating the role of upper regions of pin fins in heat transfer. This observation is particularly valid for fin height of 1.5 mm (Figure 4.4(c)) and is not common among all configurations. This is because H=1.5 mm has favorable geometrical characteristics i.e sufficient fin height and adequate passage volume above pin fins. As fin height increases beyond the optimum value of 1.5 mm, it is observed that upper regions of the pin fin cross section do not play an important part in heat transfer, as evident by the temperature values.

4.5 Performance Parameters vs Reynolds number for Varying Heat Flux

Effects of Reynolds number and heat flux on performance parameters need to be investigated. Reynolds number and heat flux are two fundamental parameters that influence the design and operation of a microchannel heat sink. Reynolds number determines the behavior of flow, within a MCHS. On the other hand, the value of heat flux determines the value of temperature gradient required for heat transfer. For a constant value of heat transfer coefficient 'h' and surface area, higher the value of heat flux, higher is the value of temperature gradient needed for heat transfer. Figure 4.5 presents plots of performance parameters against Reynolds number for varying values of heat flux. Fin height 'H' is 1.5 mm while fin thickness 'X' is 0.4 mm. The performance parameters are (a) base temperature, T_b, (b) Nusselt number, $\overline{Nu}$, (c) pressure drop ΔP and (d) thermal performance factor, ψ. The values of heat flux vary from 75-150 kW/m^2. Heat flux and Reynolds number show profound effects on performance parameters. As value of heat flux

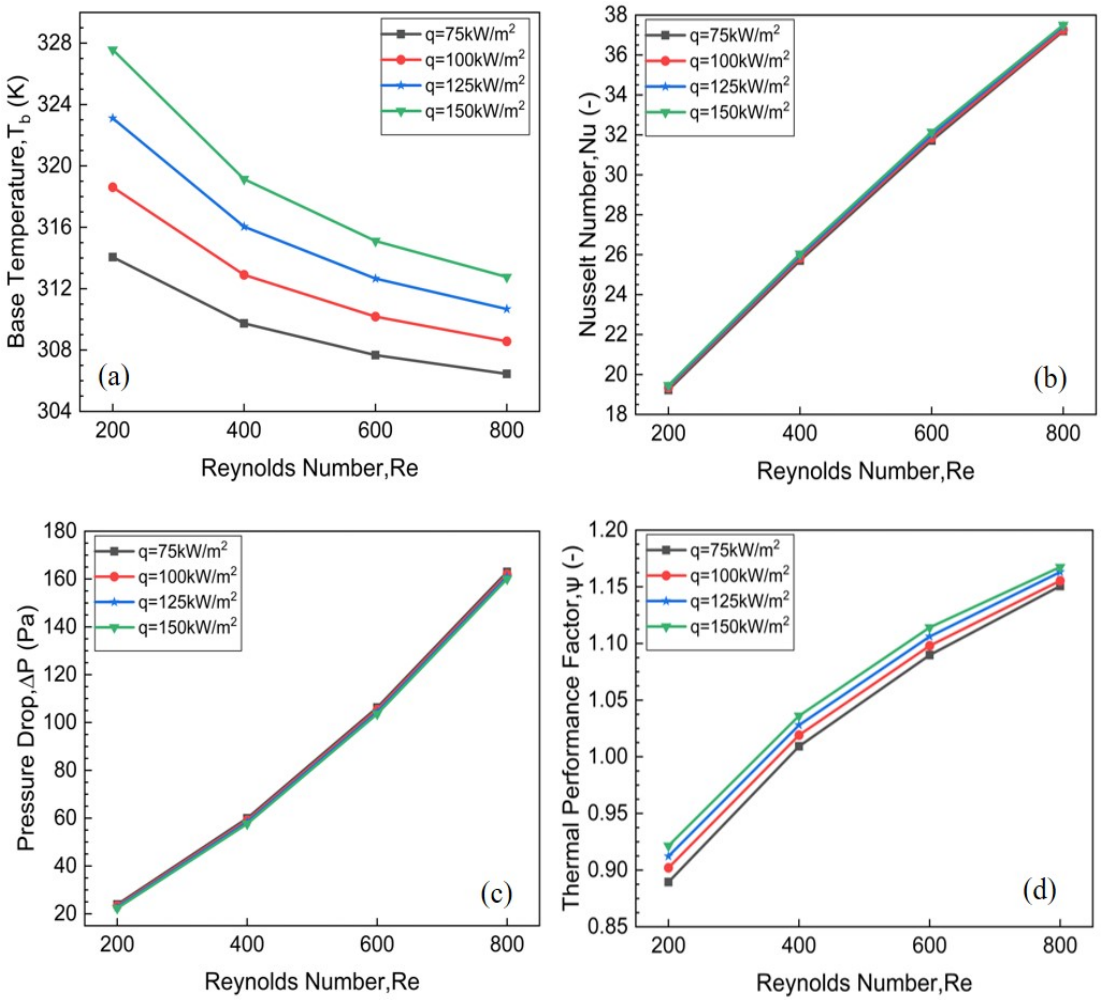

FIGURE 4.5: (a) Base temperature, (b) Nusselt Number, (c) pressure drop and (d) TPF vs Reynolds for changing heat flux for fin height of 1.5 mm and thickness of 0.4 mm

increases, base temperature of the heat sink also increases. Increasing Reynolds number decreases the value of T_b, for all heat flux values, depicting higher heat transfer. The highest value of base temperature, T_b is recorded for heat flux of 150 kW/m^2 i.e 327.5 K. Conversely, the lowest value is recorded for heat flux of 75 kW/m^2 i.e 306.4 K. Moreover, the highest value is recorded for Reynolds number of 200 while the lowest is recorded for Reynolds number of 800. At Reynolds number of 200, the effect of heat flux on T_b is maximum, depicted by larger difference in T_b values. This difference gradually starts to decrease as Reynolds number is increased. An increase in Reynolds number dampens the individual effects of heat flux on base temperature, T_b.

Figure 4.5 (b) shows that heat flux has negligible effects on average Nusselt number, $\overline{Nu}$. This is because Nusselt number is a ratio of convection and conduction.

Irrespective of the change in base temperature T_b due to varying heat flux, $\overline{Nu}$ remains almost same, since it takes both convection and conduction in to the account, simultaneously. Furthermore, Nusselt number increases with increasing Reynolds number. The reason being that convection heat transfer coefficient increases with increasing Reynolds number. Pressure drop is a strong function of Reynolds number.With increase in Reynolds number, pressure drop increases in a nonlinear profile. Pressure drop is not a function of heat flux as shown in Figure 4.5 (c). For varying values of heat flux, negligible difference in pressure drop values is recorded. The negligble difference which occurs is due to the change in the properties of the working fluid with temperature,in the flow domain.

Figure 4.5 (d), represents effects of heat flux on thermal performance factor, ψ. There is relatively small difference among ψ values, with change in heat flux. At Reynolds of 200, this difference is more profound. As Reynolds number increases, difference among ψ values reduces substantially. At Reynolds of 800, the difference among ψ values is almost negligible. This is because at lower Reynolds number, effects of heat transfer coefficient 'h' on ψ are not dominant. As Reynolds number increases, heat transfer coefficient 'h' dominates the value of ψ, thus negligible difference among ψ values is recorded. Furthermore, thermal performance factor, ψ does not increase linearly with increasing Reynolds number. The highest values of ψ exist for heat flux of 150 kW/m^2 while the lowest exist for 75 kW/m^2, at respective Reynolds numbers. This is because as heat flux increases, $\overline{Nu}$ also increases. Increase in Nusselt number values indirectly increases the value of ψ.

4.6 Effects of Varying Reynolds Number on Velocity Contours

Influence of Reynolds number on velocity profile needs to be investigated. Heat sink inlet velocity is a function of Reynolds number only. With an increase in Reynolds number inlet velocity increases which significantly changes the velocity profile and its effects on heat transfer. Figure 4.6 presents velocity contours at zx and xy planes at Reynolds of (a) 200, (b) 400, (c) 600 and (d) 800 for fin height of

1.5 mm and thickness of 0.4 mm (optimum configuration). Heat flux value remains constant at 150 kW/m^2. Change in Reynolds number affects the flow behavior in a profound manner. Understandably, Figure 4.6 (a) represents lowest velocity values while Figure 4.6 (d) represents the highest velocity values. The highest velocity value is 0.49 m/s while the lowest is 0.14 m/s. In heat transfer problems, increasing Reynolds number always positively affects heat transfer, owing to the increase in convective heat transfer coefficient. Flow disturbances also increase with increasing Reynolds which are beneficial for heat transfer.

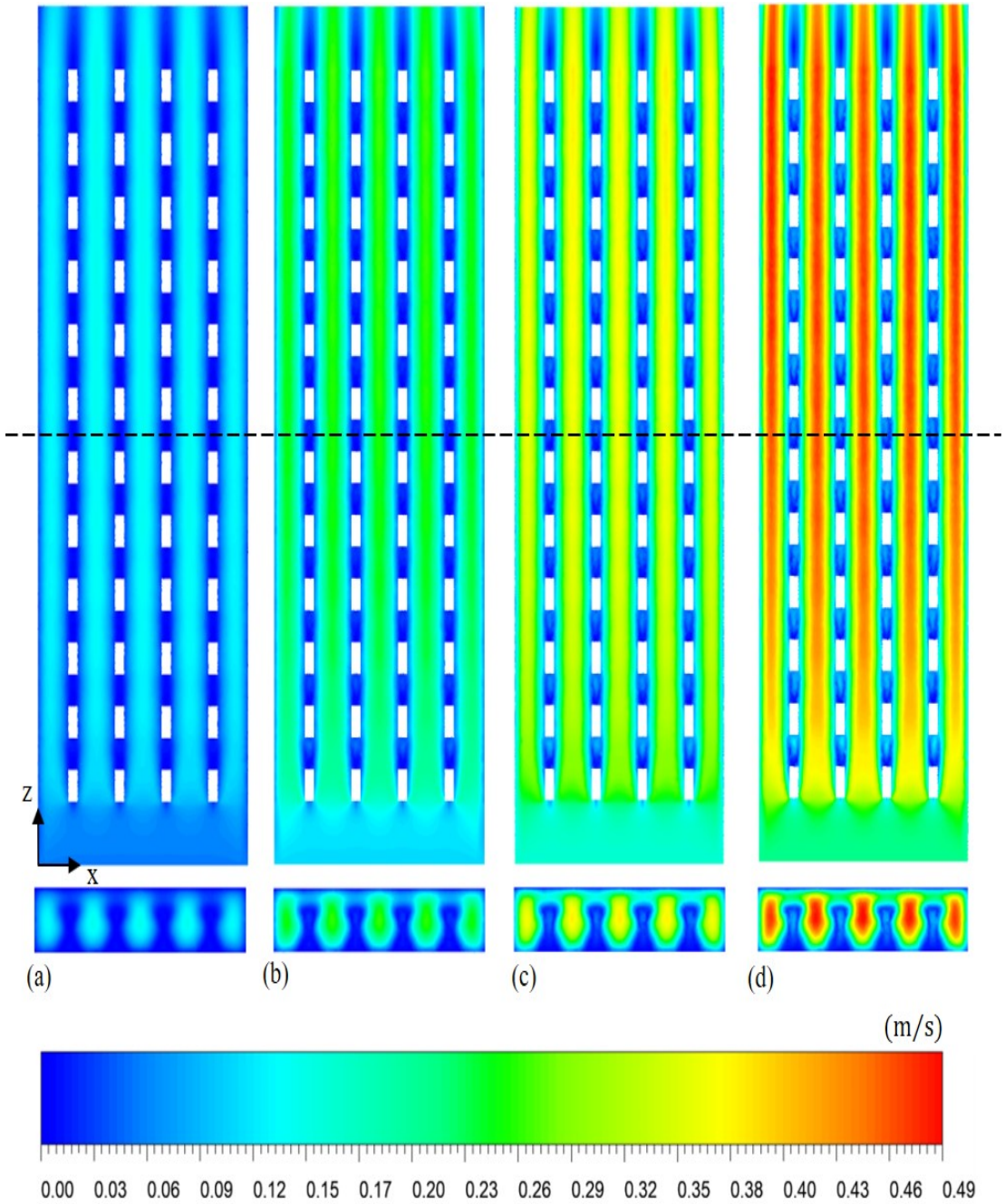

FIGURE 4.6: Velocity contours for varying Reynolds number

4.7 Effects of Varying Reynolds Number: Temperature Contours

Temperature profile under the influence of Reynolds number needs to investigated. Heat transfer coefficient which is a function of Reynolds number, dominates the behavior of temperature profile. Figure 4.7 presents temperature contours at zx and xy planes at Reynolds of (a) 200, (b) 400, (c) 600 and (d) 800 for fin height of 1.5 mm and thickness of 0.4 mm (optimum configuration). Heat flux value remains constant at 150 kW/m^2. Temperature profile is highly dependent on the value of Reynolds number. The intensity and degree of forced convection is dictated by Reynolds number. Figure 4.7 (a) represents the highest value of coolant temperature i.e 330.9 K. Conversely, Figure 4.7 (d) represents the lowest temperature value of 314.3 K. Irrespective of the value of Reynolds number, within the heat sink, higher values of temperature are encountered at the last part (extreme downstream location) of heat sink. This is because at this location of heat sink, coolant temperature is already high as a consequence of heat transfer. As a result, temperature gradient between coolant and fin surface at this location is very small, resulting in significantly less heat transfer.

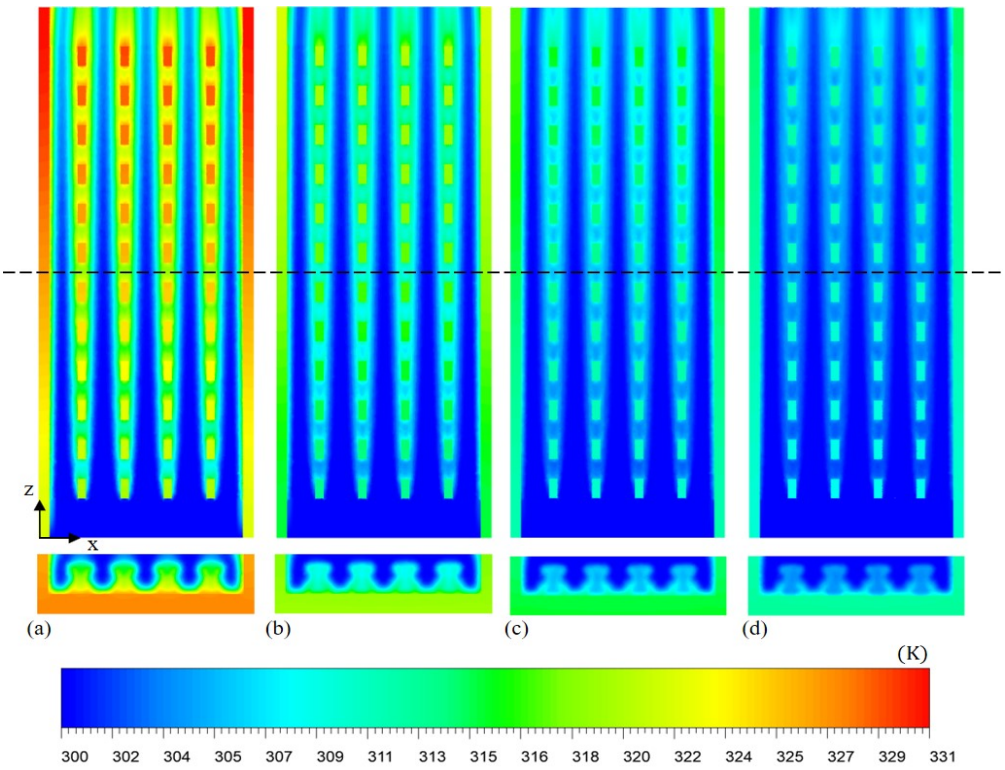

FIGURE 4.7: Temperature contours for varying Reynolds number

4.8 Effects of Varying Heat Flux on Temperature Contours

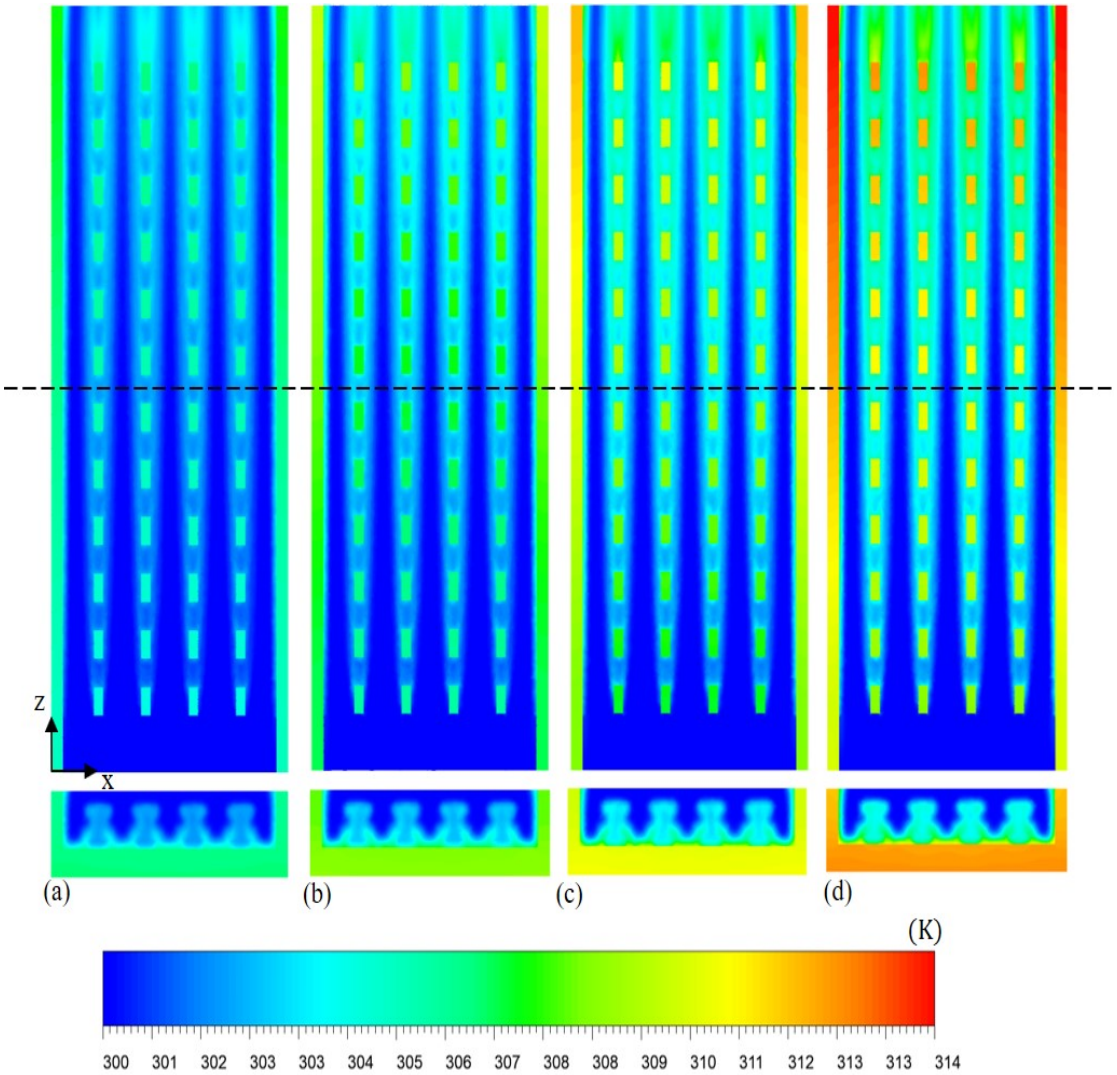

FIGURE 4.8: Temperature contours for varying heat flux

It is important to analyze the effects of heat flux on temperature profile. A higher value of heat flux results in higher temperatures within the heat sink. This significantly affects the behavior of temperature profile throughout the flow domain. Figure 4.8 presents temperature contours at zx and xy planes at heat flux values of (a) 75, (b) 100, (c) 125 and (d) 150 kW/m^2 for fin height of 1.5 mm and thickness of 0.4 mm (optimum configuration). Reynolds number is held constant at the value of 800. Within this heat sink, heat flux is the only source of energy. The magnitude of this heat energy (applied at the base), promptly translates itself in to a temperature distribution, at the heat sink. For a constant Reynolds

number, higher the value of heat flux, higher will be the temperature. Figure 4.8 (a) represents the lowest temperature value of 307.2 K. Conversely, Figure 4.8 (d) represents the highest temperature value of 312.7 K. For the same value of heat transfer coefficient 'h', as the value of heat flux increases, more heat transfer is required to maintain lower temperature within the flow domain. Since heat transfer cannot be increased by keeping heat transfer coefficient 'h' and surface constant, temperature within the heat sink rises as a consequence. Thus, with increase in heat flux values, temperatures within the flow domain increase correspondingly. Change in the value of heat flux does not alter the behavior of the velocity profile, as inlet velocity is not a function of heat flux. In this regard, velocity profile for all the above-mentioned cases, remains same.

4.9 Velocity Streamlines

Velocity streamlines provide a unique graphical representation of flow interaction with solid surfaces, within the flow domain. This graphical representation provides details of underlying flow physics within a velocity profile. Thus, it is of importance to investigate velocity streamlines of specific geometrical cases. Figure 4.9 presents velocity streamlines at two different planes for fin heights of 1 mm and 1.75 mm respectively. Fin thickness, X is 0.4 mm. Reynolds number is 800 while the value of heat flux is 150 kW/m^2. Figure 4.9 (a) shows velocity streamlines at xy plane (z=13.5 mm from inlet) for fin height of 1 mm while Figure 4.9 (b) shows velocity streamlines at xy plane for fin height of 1.75 mm.Figure 4.9 (b) and (d) show velocity streamlines at zx plane for fin heights of 1 mm and 1.75 mm respectively.Fin heights of 1 mm and 1.75 mm are chosen for their minimum and maximum values of velocity respectively. Figure 4.9 (a) shows formation of a vortex pair behind each pin fin cross section.Each vortex pair recirculates the flow behind pin fin cross sections. Right above pin fin cross sections, it can be seen that velocity magnitude increases and reaches its peak value at a certain height from pin fins. For fin height of 1 mm, velocity magnitude is 0.35 m/s. Figure 4.9 (c) shows a completely different velocity profile. Instead of one vortex pair, there are two vortex pairs behind each pin fin cross sections. This is because unlike H=1

mm, for H=1.75 mm coolant has enough space behind the pin fin cross section to interact with solid surface, recirculate and form two vortex pairs. Unlike fin height of 1 mm, velocity magnitude reaches its peak value in the lateral (x) direction. For H=1.75 mm, formation of two vortex pairs indicate enhanced flow mixing and better heat transfer. Furthermore, a single vortex pair for H=1 mm indicates recirculation of less intensity which results in less heat transfer.

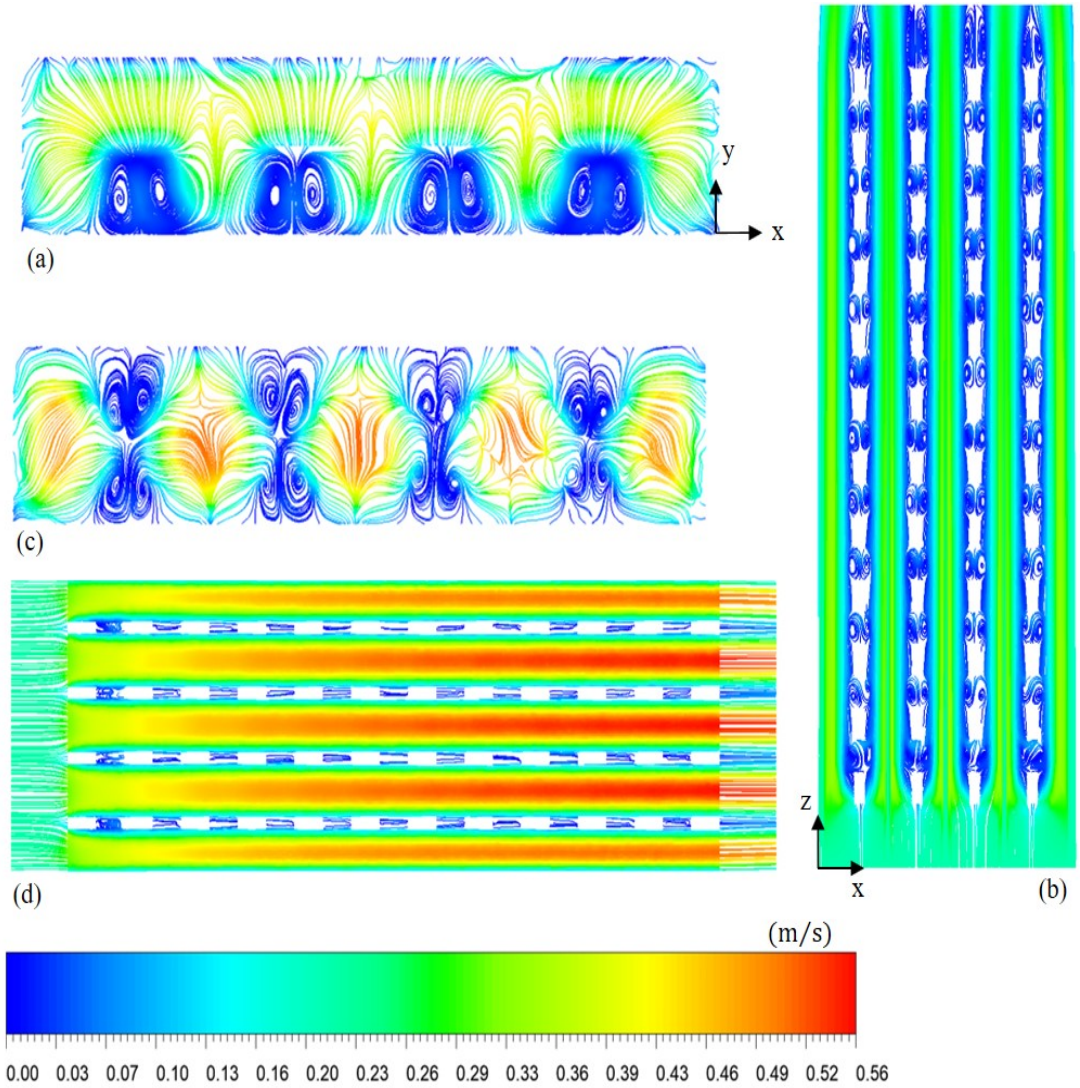

FIGURE 4.9: Velocity streamlines for fin heights of 1 mm and 1.75 mm

4.10 Thermal Resistance

Thermal resistance is analogous to electrical resistance. An electrical resistance provides resistance to the current flow. On the other hand, thermal resistance

provides resistance to the heat flow. In an electrical problem, voltage difference is the driving force for current while in a heat transfer situation, temperature difference is the driving force for heat flux. Higher the value of thermal resistance, lower will be the value of transferred heat. For conjugate heat transfer problems, following is the formula of thermal resistance,

$$R_{th} = \frac{T_{base,avg} - T_{in}}{q'' \times A_{base}} \tag{4.1}$$

Where R_{th} is the thermal resistance. $T_{base,avg}$ is the average temperature of the

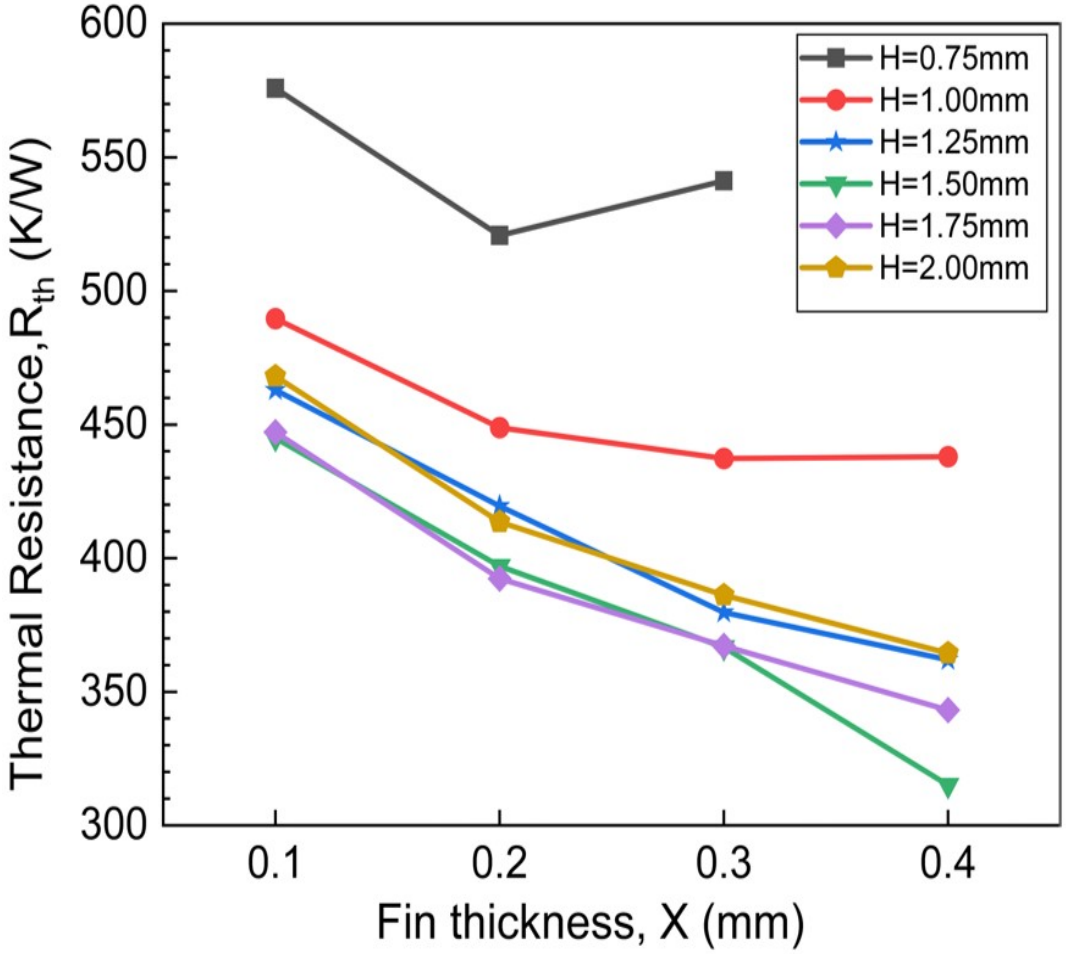

FIGURE 4.10: Thermal resistance against fin thickness for varying fin heights

base where heat flux is applied. T_{in} is the inlet temperature. A_{base} is the area of the base while q" is the heat flux applied at the base of heat sink.

Figure 4.10 presents plot of thermal resistance, R_{th} against fin thickness 'X' for varying fin heights 'H', at Reynolds number of 800 and heat flux value of 150 kW/m^2. Fin thickness 'X' varies from 0.1-0.4 mm while fin height 'H' varies from

0.75-2 mm. Thermal resistance is represented in units of Kelvins per Watt. As shown in Figure 4.10, the highest thermal resistance value of 575.8 K/W exists for H=0.75 mm and X=0.1 mm. On the other hand, the lowest thermal resistance value of 315.0 K/W exists for H=1.5 mm and X=0.4 mm. A lower value of thermal resistance is desired. The trend of base temperature 'T_b' plot and thermal resistance 'R_{th}' plot are identical. This is because thermal resistance is dependent on only one variable i.e base temperature T_b.

Chapter 5

Effects of Fin Orientation on Hydro-Thermal Performance

Based on the results of Chapter 4, it is realized that there exists a need to further investigate the interaction and behavior of a pin fin with the coolant. Flow characteristics of the coolant are dominated by its interaction with the pin fin. In addition, heat transfer in a pin fin microchannel heat sink is directly influenced by the cross section of the pin fin. Pin fin cross section incorporates the effects of both height 'H' and thickness 'X'. Change in H and X alter the flow behavior and thus hydro-thermal performance of MCHS. In this context, it is realized that each pin fin cross section induces a unique flow behavior in the heat sink. The objective of this chapter is to achieve favorable flow behavior and enhance hydro-thermal performance of a MCHS by orienting the pin fins at different orientations. Four angled configurations are created, named C-1, C-2, C-3 and C-4 respectively. For each configuration, orientation of 15°-90° is considered. Angle 'θ' changes with an increment of 15°. All 4 angled configurations are created for the optimum case of H=1.5 mm and X=0.4 mm. Optimum case is considered as the reference case. Performance parameters are plotted and results are analyzed in the context of the reference case. Analysis of effects of pin fin orientation holds importance since surface area remains same irrespective of configuration type or orientation type. Constant surface area helps determine other causes of increase in heat sink performance.

5.1 Geometry

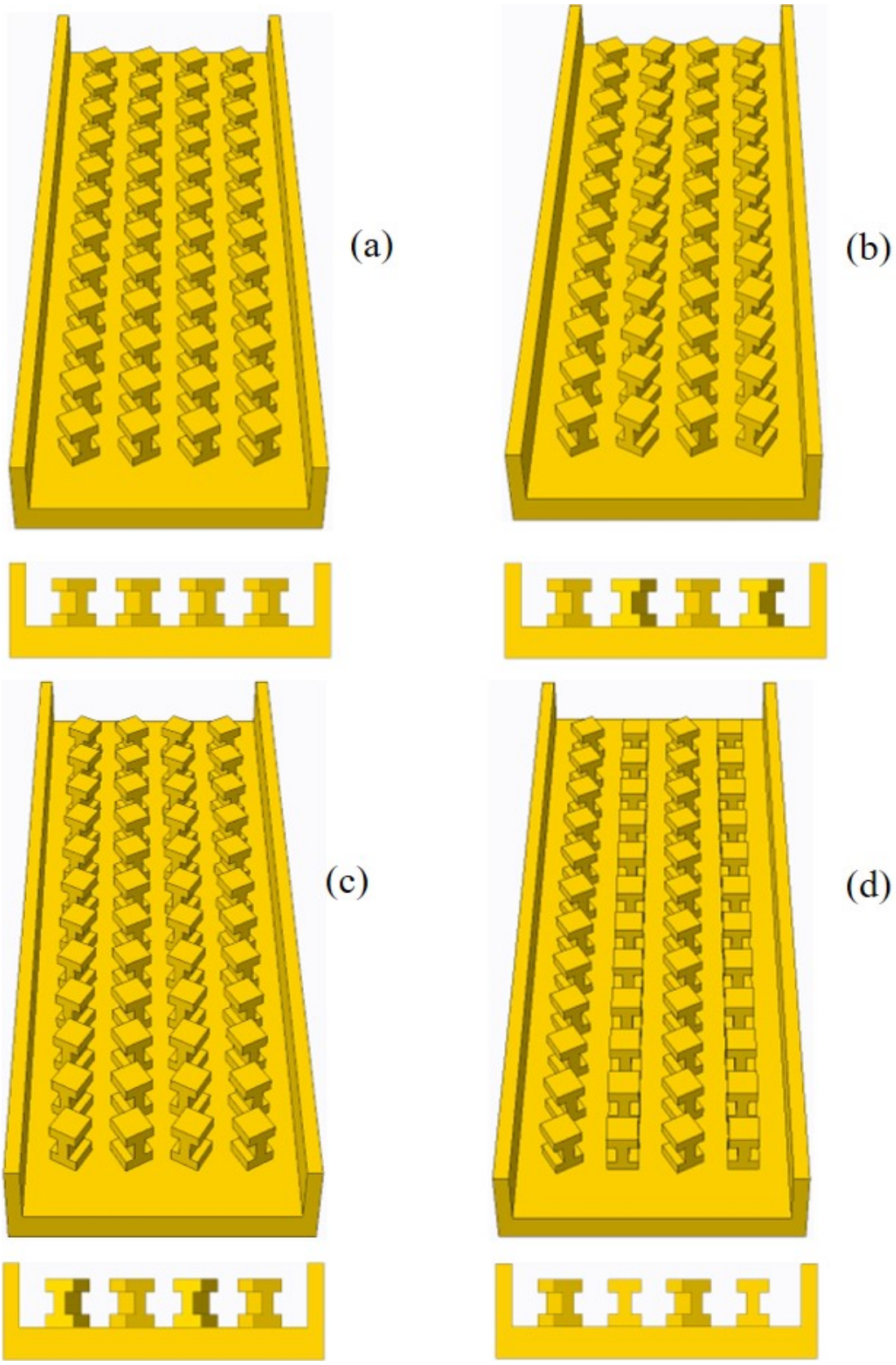

FIGURE 5.1: Geometry representing angled cases, (a) Configuration-1, (b) Configuration-2, (c) Configuration-3, (d) Configuration-4, at θ= 30°

Figure 5.1 presents detailed geometrical description of the microchannel heat sink with 4 different angled configurations, at an angle of 30°. For each geometric configuration, both front and cross-sectional views are presented. Configuration-1 represented by Figure 5.1 (a) has all the pin fins at the same orientation. Configuration-2 and 3 are represented by Figure 5.1 (b) and (c) respectively. Configuration-4 represented by Figure 5.1 (d) has two fin rows at an angle and the other two fin rows without an angle.

5.2 Mesh

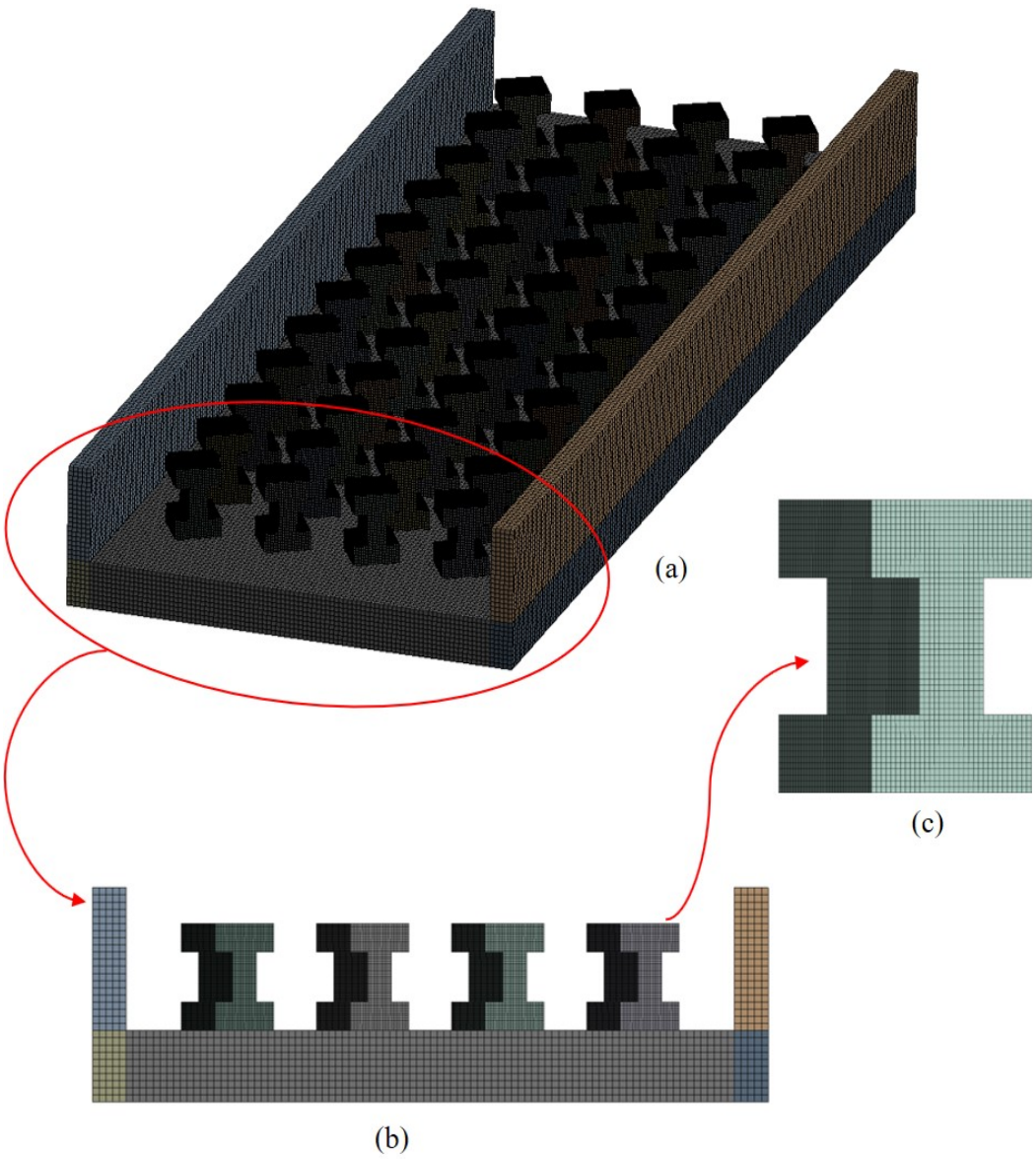

FIGURE 5.2: Representation of mesh for angled cases, (a) isometric view, (b) heat sink cross-section, (c) pin fin cross section

Figure 5.2 presents mesh of an angled case with different views, (a) isometric view, (b) cross sectional view and (c) individual pin fin cross-section. Configuration-1, angle of 30° has been chosen for this representation. Number of elements for this mesh are 3.0 million. Number of mesh elements on the pin fin cross section thickness 'X' are 13.

5.3 Performance Parameters v/s Angle 'θ'

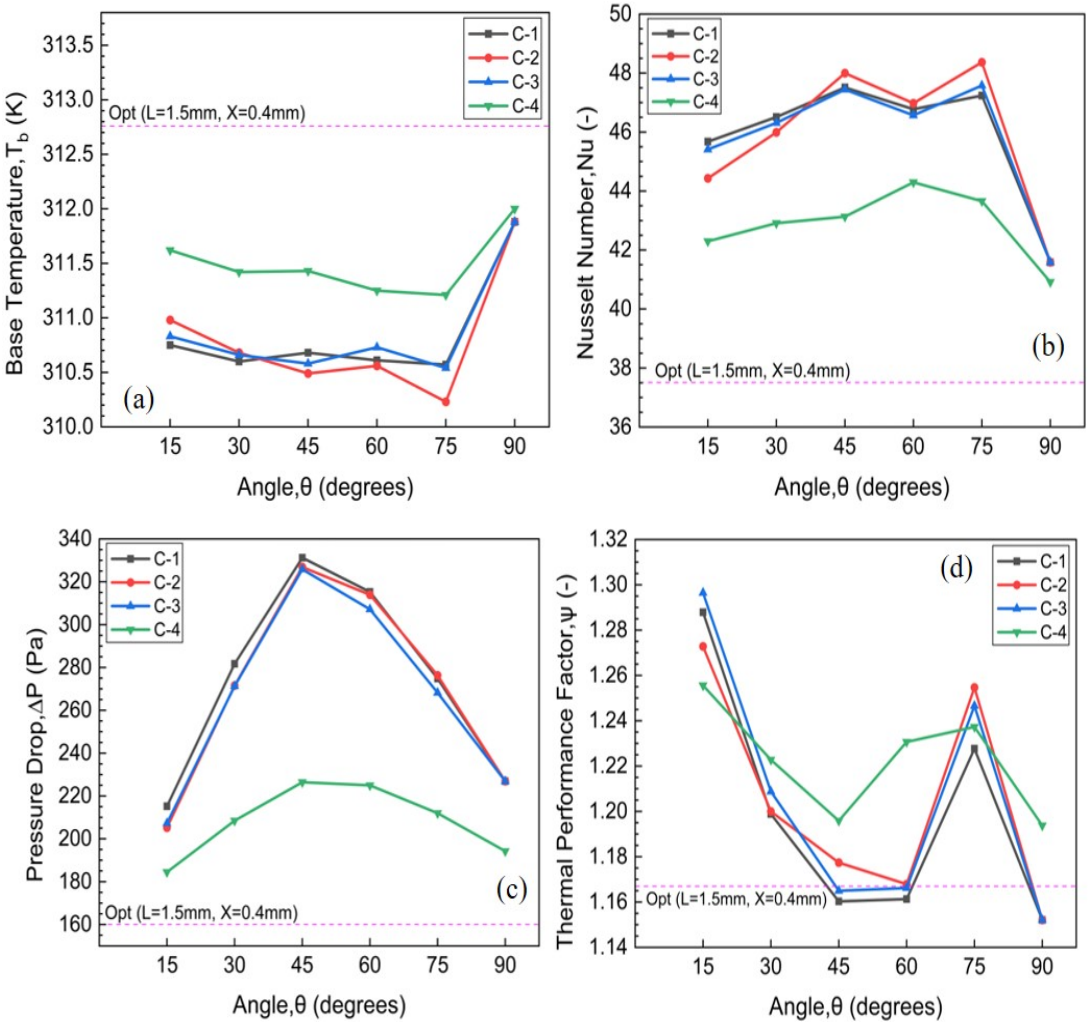

FIGURE 5.3: Performance parameters v/s Angle 'θ', (a) base temperature, (b) Nusselt Number, (c) pressure drop and (d) TPF

In order to investigate the effects of pin fin orientation on performance parameters, line plots are created for each performance parameter against orientation 'θ'. Figure 5.3 presents plots of performance parameters against angles in degrees for angled cases with different configurations, at Reynolds number of 800 and heat

flux value of 150 kW/m^2. As mentioned before, all angled cases are solved for the optimum case i.e fin height 'H' of 1.5 mm and fin thickness 'X' of 0.4 mm.The optimum case (H=1.5 mm, X=0.4 mm) results are presented as a reference line in all the plots of Figure 5.3. Reference line is drawn for comparative purposes. Furthermore, this reference line represents benchmark values of respective performance parameters. Comparison with these benchmark values will indicate improvement or reduction in the hydro-thermal performance.

In Figure 5.3 (a), base temperature, T_b is plotted. As angle is increased, T_b decreases, till 75°. After this, at the angle of 90°, T_b increases. This trend is common for all 4 angled configurations. Reference value is 312.7 K. All data points on Figure 5.3 (a) lie below this reference value. The difference between the highest and the lowest value of T_b is less than 3 K. On the graph, the highest value of base temperature is 312.0 K for C-4, θ=90°. The lowest value of T_b is 310.2 K for C- 2, θ=75°.For all angled configurations, an angle of 75° represents a favorable pin fin orientation, in the context of base temperature. The trend of line plot changes significantly from 75° to 90°. This is because at θ=90°, pin fin cross section facing the flow is not an I-shape. Instead, the cross section becomes more like a square cross section with area removed in the inward direction. This cross-section provides unfavorable flow characteristics for heat transfer.

Figure 5.3 (b) shows that the value of Nusselt number, $\overline{Nu}$ increases as angle is increased, till 45°. After 45°, the value of $\overline{Nu}$ decreases, increases and then decreases again, in succession till 90°. This trend is common for all 4 angled configurations. Reference value is 37.5. All data points on Figure 5.3 (b) lie well above this reference value. The highest value of Nusselt number is 48.3 for C-2, θ=75°. The lowest value of $\overline{Nu}$ is 40.9 for C-4, θ=90°. It is important to note that the lowest value of $\overline{Nu}$ (40.9) is 8.3% larger than the reference value. This represents that even at the lowest value of $\overline{Nu}$, an improvement is recorded compared to the reference case. Furthermore, for all angled configurations except Configuration-4, an angle of 75° represents a favorable pin fin orientation, in the context of Nusselt number. Figure 5.3 (c) shows that the value of pressure drop, ΔP increases as angle is increased, till 45°. Afterwards ΔP decreases till 90°. Peak pressure drop is achieved at an angle of 45°. These trends are common

for all 4 angled configurations. Reference value is 160.0 Pa. All data points on Figure 5.3 (c) lie well above this reference value. This shows that pin fin orientation significantly increases the value of ΔP irrespective of configuration or angle, compared to the reference case. This is because more surface area of a pin fin faces directly towards the incoming flow. Furthermore, pin fin orientations cause the flow to accelerate at certain locations within the flow domain. For instance, certain angled configurations result in a converging flow which result in higher velocity values. Higher velocity values result in higher pressure drops. The highest value of ΔP is 331.2 Pa for C-1, θ=45°. The lowest value of ΔP is 184.4 Pa for C-4, θ=15°. For all angled configurations, an angle of 15° represents a favorable pin fin orientation, in the context of pressure drop.

Figure 5.3 (d) shows that the value of thermal performance factor, ψ decreases as angle is increased, till 45°. From 45° to 60°, the change is negligible. From 60° to 90°, ψ increases then decreases, respectively. This trend is common for all angled configurations except Configuration-4. For Configuration-4, there is a significant rise in ψ value from 45° to 60°. Reference value for ψ is 1.16. The highest value of ψ is 1.29 for Configuration-3, angle of 15°. For all angled configurations, an angle of 15° represents a favorable pin fin orientation, in the context of thermal performance factor.

5.4 Configuration-3 -Velocity Contours at Orientations of 15°-90°

Investigation of temperature and velocity contours is important to visualize the flow physics and understand the flow characteristics of different pin fin orientations. Figure 5.4 presents velocity contours at xz plane(mid-fin) for Configuration 3 at angles of (a) 15°, (b) 20°, (c) 45°, (d) 60°, (e) 75° and (f) 90°. Reynolds number is 800 while heat flux is 150 kW/m^2. Contours of velocity are presented for Configuration-3 as this configuration yields the highest value of ψ i.e 1.29 for an angle of 15°. Highest velocity magnitude of 0.66 m/s is recorded, for the angle of 45°. For the angle of 90°, lowest velocity magnitude of 0.54 m/s is recorded.

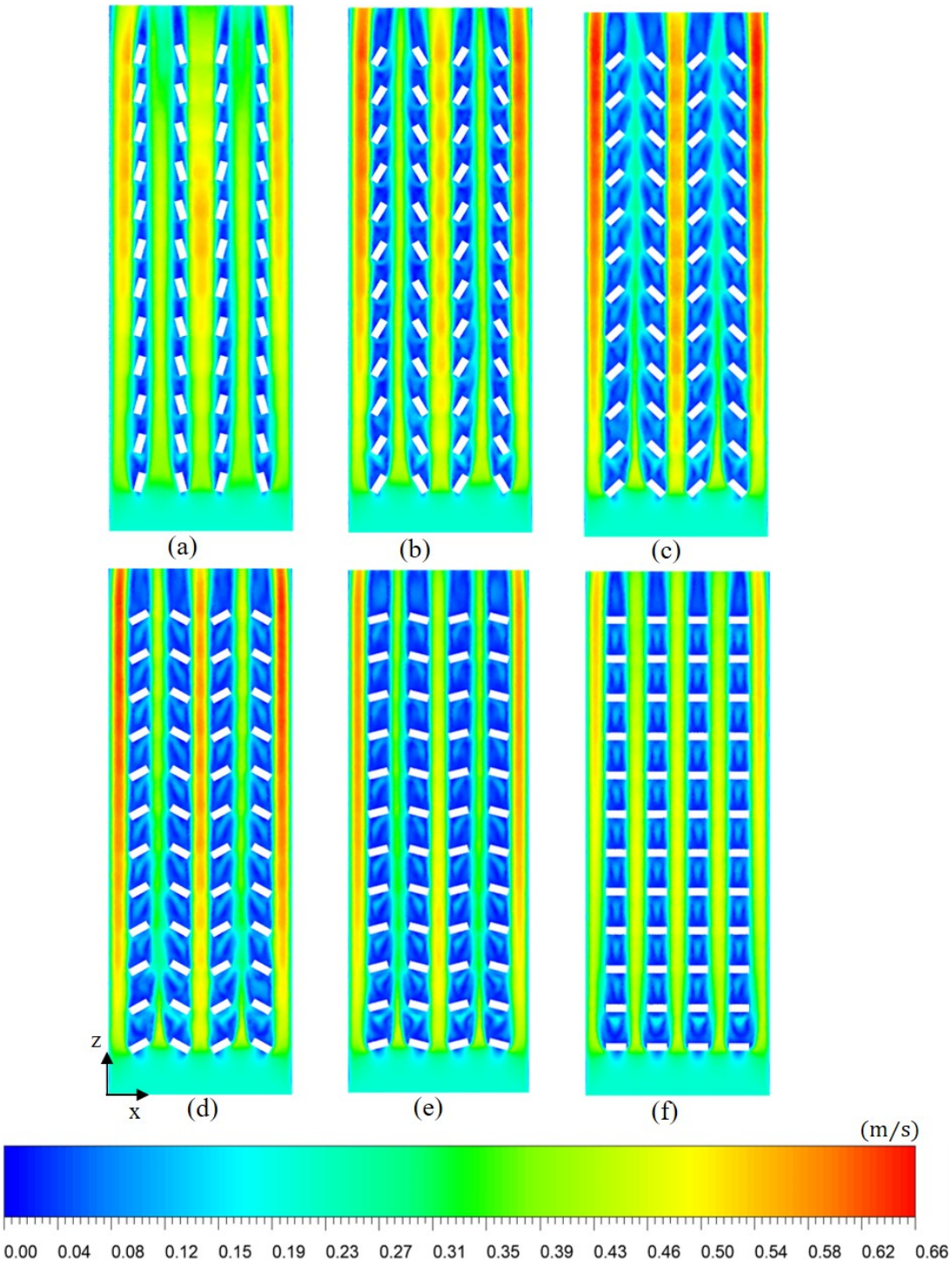

FIGURE 5.4: Velocity contours at multiple orientations for Configuration-3

As flow moves downstream, flow regions with the high velocity are recorded in the channels. These flow regions of high velocity exist only adjacent to the sidewalls and in the middle channel. As angle increases from 15° to 45°, velocity magnitude increases. Afterwards, from 45° to 90°, velocity magnitude starts to decrease. As θ is increased, area of the adjacent passage is reduced. To conserve mass, velocity magnitude increases in that respective channel. Channels between the pin fins

(except middle channel) have significantly lower values of velocity. This is because of the fact that passage area for flow is increased in these channels. In terms of thermal performance factor ψ, for all configurations, θ=15° performs best while θ=90° has the worst performance. This is because 15° orientation has not only lower base temperature but also lower pressure drop values, for all configurations. On the other hand, 90° has lowest pressure drop values but also the highest base temperature values, for all configurations. Due to this reason 15° exhibits the highest hydro-thermal performance.

5.5 Configuration-3 -Temperature Contours at Orientations of 15°-90°

Figure 5.5 presents temperature contours at xz plane(mid-fin) for Configuration-3 at angles of (a) 15°, (b) 30°, (c) 45°, (d) 60°, (e) 75° and (f) 90°. Reynolds number is 800 while heat flux is 150 kW/m^2.Highest temperature value of 313.4 K is recorded for the angle of 90°.On the other hand, lowest temperature value of 311.3 K exists at an angle of 15°. Temperature value rises as θ is increased, from 15° to 60°. At θ=75°, temperature drops by a small fraction before rising again at the angle of 90°. Middle channel and channels adjacent to the walls are dominated by regions of lower temperature values. This is because of higher velocities in these regions. Higher velocity values yield higher convective heat transfer coefficient values.

Channels between the pin fins (except middle channel) have regions of higher temperature values. These regions of high temperature start to expand as flow passes downstream, in the last half of heat sink. Pin fins at a particular orientation dissipate more heat than pin fins that are unoriented. From 15° to 75°, the maximum difference in temperature values for any two orientations is 0.5 K. This difference is increased to a value of 2.1 K when 90° orientation is also taken in to account. This observation indicates that flow mixing is essential for heat dissipation. A pin fin which has its face normal to the incoming flow (90°orientation), undergoes significantly less flow mixing.

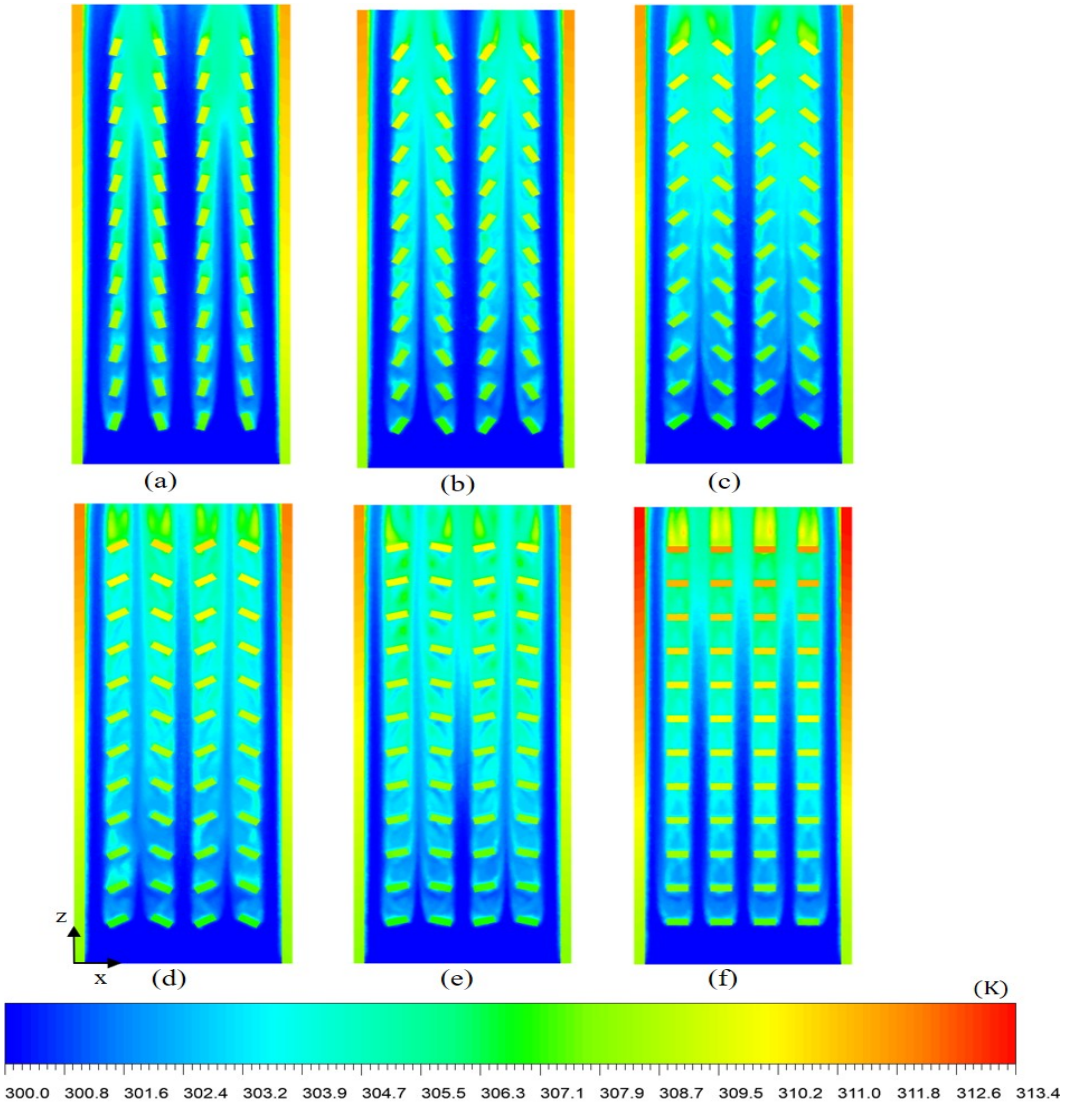

FIGURE 5.5: Temperature Contours at multiple orientations for C-3

5.6 15°-Velocity Contours for All Configurations

Velocity and temperature contours at an orientation of 15° are chosen for representation because at 15°, highest value of ψ is achieved i.e 1.29, for Configuration-3.Figure 5.6 presents velocity contours at xz plane(mid-fin) for (a) Configuration-1, (b) Configuration-2, (c) Configuration-3 and (d) Configuration-4, at an orientation of 15°. Reynolds number is 800 and heat flux is 150 kW/m^2. Each angled configuration has a unique velocity profile. Highest velocity magnitude of 0.57 m/s is recorded for Configuration-4. On the other hand, lowest velocity magnitude of 0.54 m/s is recorded for Configuration-2. The difference between these two values is not significant i.e a difference of 5.2%. Based on this observation, it should be acknowledged that at θ=15°, velocity magnitude does not play a significant role in

heat transfer. Despite this, the importance and impact of velocity profile and flow behavior cannot be under estimated. Figure 5.6 (a) representing Configuration-1 has an asymmetric velocity profile. Dominant regions of low velocity exist in the left most channel. On the other hand, predominant regions of highest velocity exist in the right most channel. The in between channels have more or less same flow behavior.

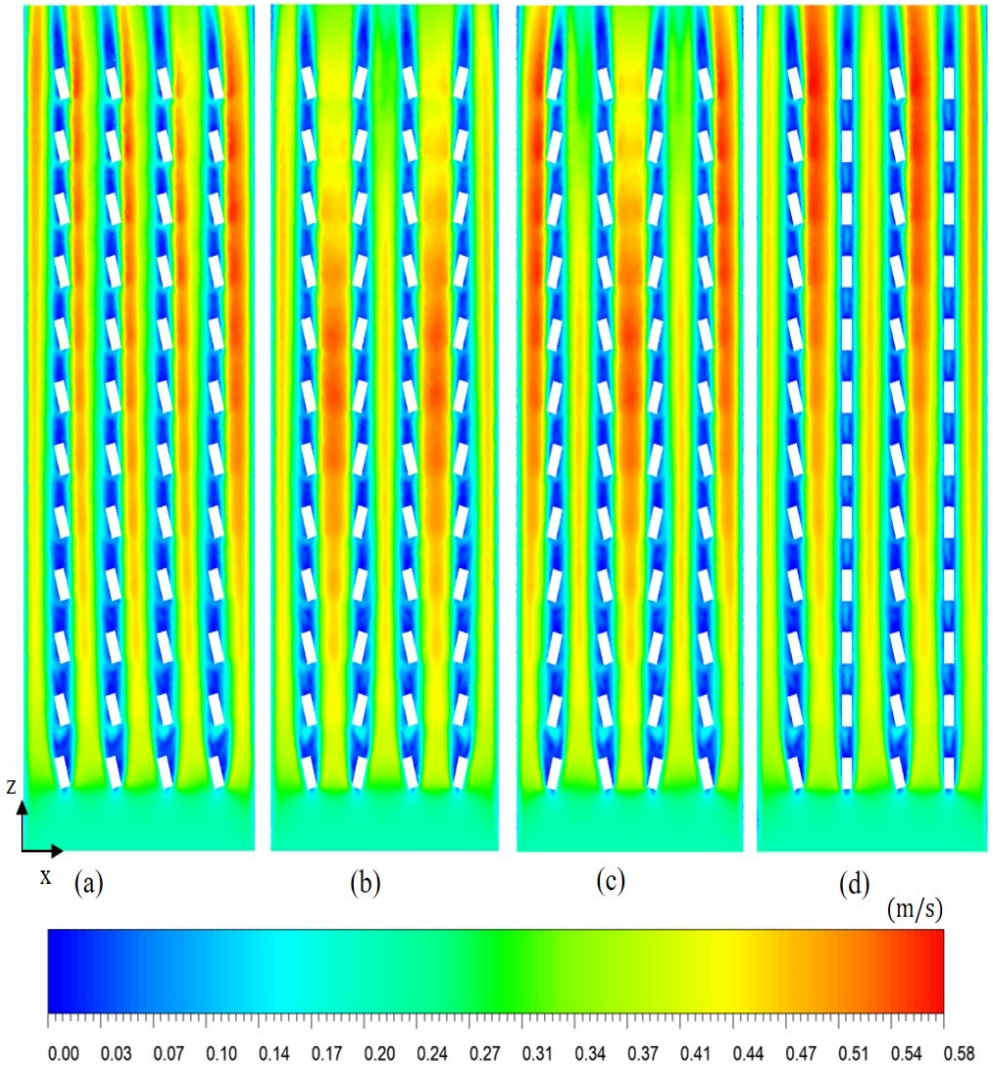

FIGURE 5.6: Velocity contours for all configurations at 15°

Configuration-2 has dominant regions of high velocity in the channels between pin fins (except middle channel). Pin fins surrounding these two channels have a converging geometric profile. However, it is important to note that these aforementioned regions tend to diminish towards the end of heat sink. Configuration-3 has only one channel where surrounding pin fins form a converging geometric profile i.e the middle channel. This middle channel along with two side wall channels

have dominant regions of high velocity magnitude. Configuration-4 also has an asymmetric velocity profile. Left side wall and adjacent fins form a diverging geometric profile leading to very low velocity regions. On the other hand, channels between pin fins (except middle channel) have high velocity values.

Within the flow domain, higher regions of velocity are favorable as base temperature 'T_b' is decreased due to increase in heat transfer coefficient 'h'. In addition, higher regions of velocity also contribute to higher pressure drop. Configuration 2 and 3 have symmetry in their velocity profiles. This results in higher values of ψ for both configurations. On the other hand, Configuration 1 and 4 have asymmetry in the velocity profiles leading to relatively low values of ψ for both configurations.

5.7 15°-Temperature Contours for All Configurations

Figure 5.7 presents temperature contours at xz plane(mid-fin) for (a) Configuration-1, (b) Configuration-2, (c) Configuration-3 and (d) Configuration-4, at an orientation of 15°. Reynolds number is chosen as 800 while heat flux is 150 kW/m^2. Highest temperature value of 312.8 K is recorded for Configuration-4. While on the other hand, lowest temperature of 311.3 K is recorded for Configuration-3. In regards to heat dissipation, Configuration-3 has the most favorable temperature profile while Configuration-4 has the least favorable. As flow passes downstream through the heat sink, it gets heated and less heat is transferred towards the end of heat sink. Heat sink channels surrounded by converging pin fin geometric profiles undergo the highest heat transfer. For C-1, all channels except the right sidewall channel have a diverging profile. Thus, relatively higher temperature values are encountered in these regions. For C-2, there are two converging and two diverging channels (including side wall channels). Furthermore, C-3 as mentioned above, has three converging channels while two diverging. C4 on the other hand has three diverging and two partially converging channels respectively. These temperature profiles directly influence the values of base temperature T_b.

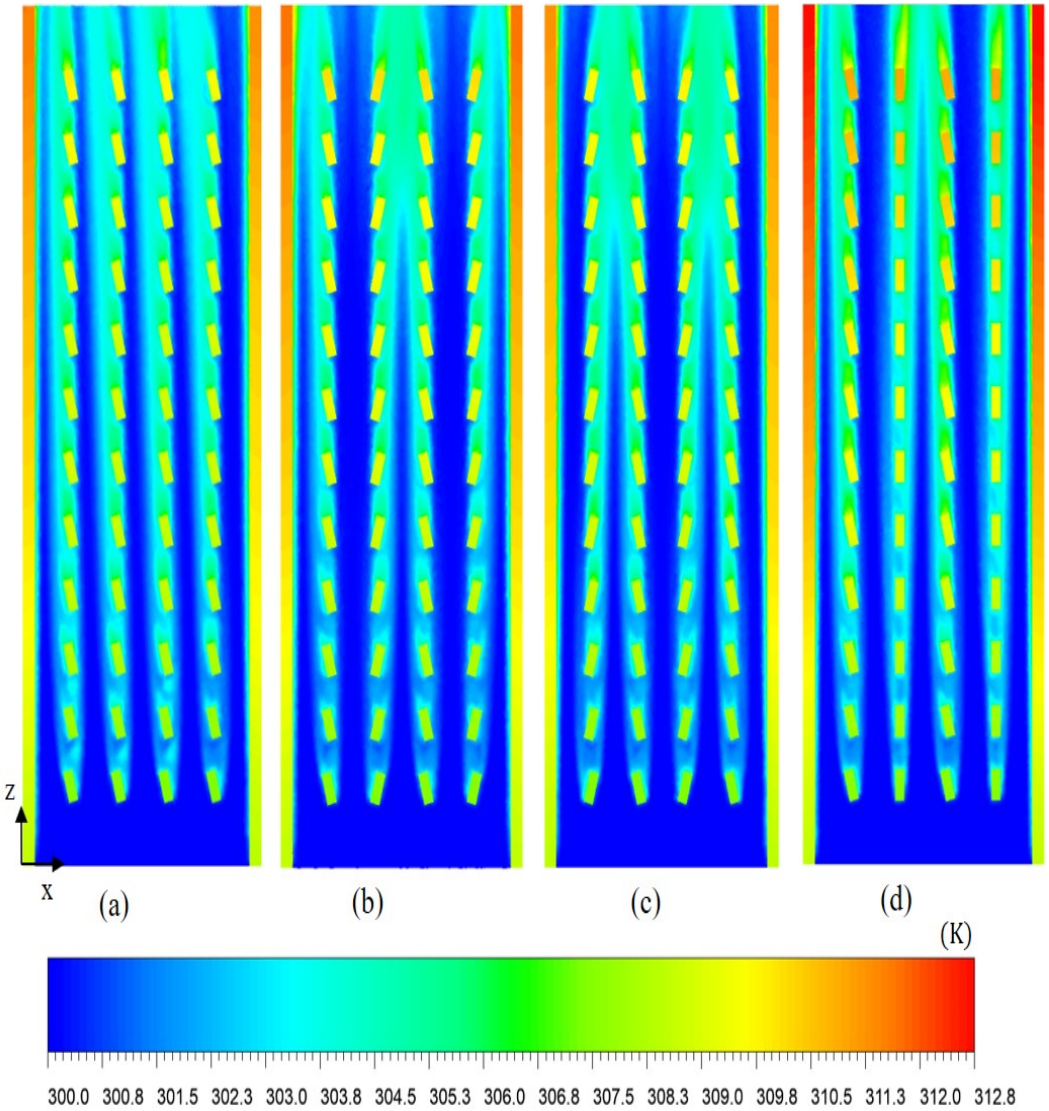

FIGURE 5.7: Temperature contours for all configurations at 15°

For instance, the values of T_b for C-2 and C-3 are relatively low and comparable. This is followed by relatively higher T_b value for C-1, followed by highest T_b value for C-4. It is thus important to realize that channel passage area dominates how heat is dissipated. There are a total of five channels in the heat sink and for better heat transfer, majority of the channels must have higher values of convective heat transfer coefficient.

5.8 75°-Velocity Contours for All Configurations

Velocity and temperature contours for 75° orientation need to be analyzed because at θ=75°, lowest values of base temperature are recorded for all configurations.

Figure 5.8 presents velocity contours at xz plane(mid-fin) for (a) Configuration-1, (b) Configuration-2, (c) Configuration-3 and (d) Configuration-4, at an orientation of 75°. Reynolds number is 800 and heat flux is 150 kW/m^2. Highest velocity magnitude of 0.59 m/s is recorded for Configuration-3. Moreover, lowest velocity magnitude of 0.51 m/s is recorded for Configuration-2. It should be noted that for 75°, velocity magnitude is higher than the velocity magnitude (highest) at 15° orientation i.e 0.57 m/s. Furthermore, it should also be recognized that the difference between the lowest velocity magnitudes is 5%, when comparing both orientations of 15° and 75°. This indicates that an angle of 75° has significant effect on flow

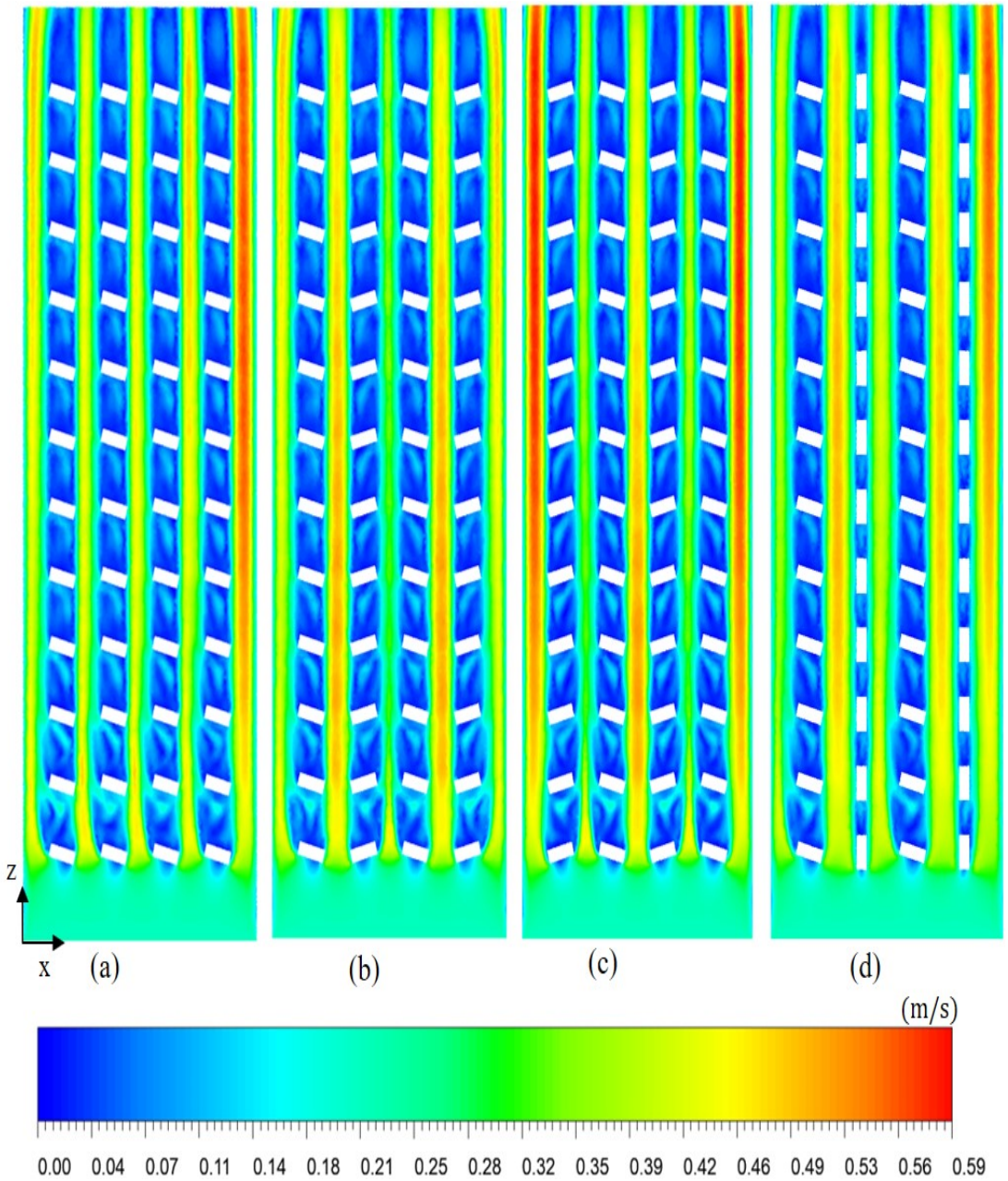

FIGURE 5.8: Velocity contours for all configurations at 75°

physics and velocity profiles. For the angle of 75°, the passage area of a diverging channel is increased while the passage area of the converging channel is decreased. This observation is common for all configurations at 75°. Comparatively, it is also evident from Figure 5.8 that converging channels have higher velocities and diverging have lower velocities. Regions of recirculation behind pin fins are much larger for 75° compared to 15° orientation. Larger wakes/regions of recirculation lead to enhanced flow mixing. Moreover, flow mixing is beneficial for heat transfer. This is the reason that lowest base temperature, T_b values are recorded at 75°, for all orientations. At orientation of 75°, pin fins occupy more space horizontally (x direction). This allows for a larger space behind the pin fins where flow is recirculated. Channels having regions of high velocity values are narrower compared to 15° orientation. On the other hand, channels with low velocity regions are much wider.

5.9 75°-Temperature Contours for All Configurations

Figure 5.9 presents temperature contours at xz plane(mid-fin) for (a) Configuration-1, (b) Configuration-2, (c) Configuration-3 and (d) Configuration-4, at an orientation of 75°. Reynolds number is 800 while heat flux value is 150 kW/m^2. While on the other hand, lowest temperature of 311.1 K is recorded for Configuration-2. Orientation of 75° provides marginally better heat dissipation as compared to orientation of 15°. This is evident by a difference of 1% in the highest temperature values when comparing both orientations. Temperature values behind the pin fins are lower comparatively because of formation of wakes and recirculation. Regardless of this, the flow gradually heats up as it passes downstream towards the outlet of heat sink.

At the outlet region, right behind the last array of pin fins, highest temperature values are achieved. At this location, flow cannot recirculate anymore. Furthermore, temperature gradient between flow and pin fins is very small. This temperature gradient is at its maximum when flow passes through the first pin fin array. Although marginally lower temperature values are encountered for 75° orientation

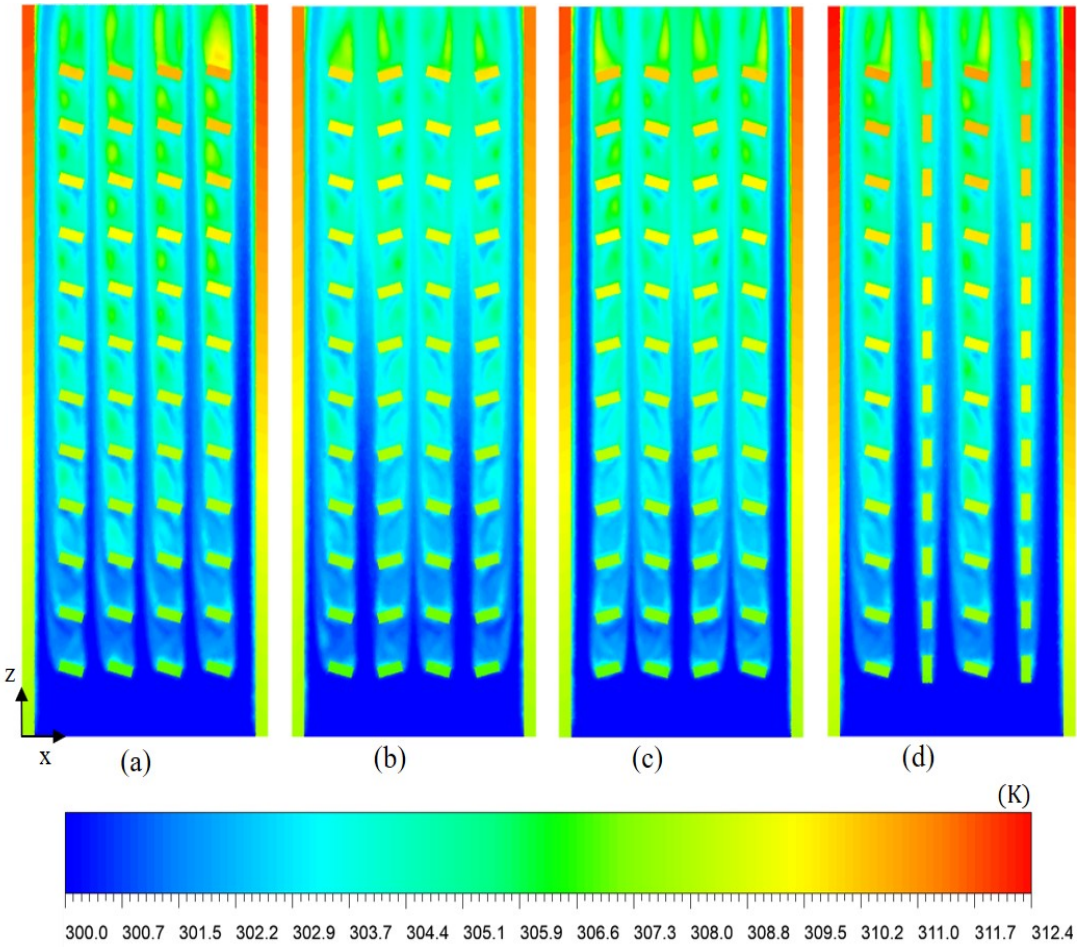

FIGURE 5.9: Temperature contours for all configurations at 75°

(when compared to 15°), the rise of pressure drop at this orientation dampens the effect of temperature on overall hydro-thermal performance. For context, the value of ψ at 15° is 1.29 while the value of ψ at 75° is 1.24.

Chapter 6

Conclusion and Future Work

• A 3-D numerical analysis has been performed on a heat sink with I-shaped pin fins. Hydro-thermal performance of the heat sink has been the primary focus. Pin fin height 'H', thickness 'X' and orientation have been varied and their effects are determined. Fin height H varies from 0.75-2 mm while fin thickness X varies from 0.1-0.4 mm. Furthermore angular orientation θ varies from 15° to 90°.

• A high density mesh has been created to accurately capture the flow physics. Mesh independence is carried out, taking into account multiple element sizes.

• Results are interpreted based on performance parameters. Performance parameters are base temperature 'T_b', Nusselt number '$\overline{Nu}$', pressure drop 'ΔP' and thermal performance factor 'ψ'.

• Initial simulations are carried out at Reynolds of 800 and heat flux of 150 kW/m^2 and an optimum case is identified. H=1.5 mm and X=0.4 mm is considered as the optimum case.

• For the optimum case, T_b=312.76K, $\overline{Nu}$=37.51, ΔP=160.05 and ψ=1.16. Base temperature ,T_b decreases as fin thickness is increased except for fin height of 0.75 and 1 mm. Nusselt number, $\overline{Nu}$ increases as fin thickness is increased except for fin heights of 0.75 and 1 mm.

• Pressure drop, ΔP increases as fin thickness 'X' is increased. Moreover ΔP also increases as fin height 'H' is increased ,except for fin height of 2 mm. Thermal

performance factor, ψ decreases with increasing fin thickness, except for fin heights of 1.25 mm and 1.5 mm.

• For the optimum case, simulations are carried out by varying Reynolds from 200-400 and heat flux from 75-150 kW/m^2.

• For a constant value of heat flux, effects of changing Reynolds number on flow physics are determined. Furthermore, on the contrary, for a constant value of Reynolds number, effects of changing heat flux on flow physics have also been determined.

• To support the quantitative results, velocity and temperature contours are created and analyzed in detail.

• For the optimum case (H=1.5 mm and X=0.4 mm), effects of pin fin orientation on the heat sink have also been investigated. In order to achieve this, 4 angled configurations are created.

• Angle θ varies from 15° to 90°, with a 15° increment. Configuration-3 at 15° performs best among all angled cases as it has the highest value of ψ i.e 1.29. Compared with reference case, this corresponds to an increase in ψ value of 29%. Thus it is established that a pin fin at particular orientation yields better hydro-thermal performance than an unoriented pin fin.

6.1 Future Recommendations

Following are the future recommendations for further research in this domain.

• Nanofluids and liquid metals (mercury etc) can be utilized to further enhance the performance of the heat sink

• Cavities and/or zigzag patterns can be included with I-shaped pin fins for further enhancement of hydro-thermal performance of the heat sink.

• Artificial intelligence and various machine learning tools should be utilized in geometric optimization of the MCHS.

- Effects of two phase heat transfer/flow boiling on heat transfer characteristics of I-shaped pin fin MCHS should be investigated in future.

Bibliography

[1] M. Guarnieri, "The unreasonable accuracy of moore's law [historical]," *IEEE Industrial Electronics Magazine*, vol. 10, no. 1, pp. 40–43, 2016.

[2] Z. Zhang, X. Wang, and Y. Yan, "A review of the state-of-the-art in electronic cooling," *e-Prime-Advances in Electrical Engineering, Electronics and Energy*, vol. 1, p. 100009, 2021.

[3] D. B. Tuckerman and R. F. W. Pease, "High-performance heat sinking for vlsi," *IEEE Electron device letters*, vol. 2, no. 5, pp. 126–129, 1981.

[4] G. Ribatski, L. Cabezas-Gómez, H. Navarro, and J. Saíz-Jabardo, "The advantages of evaporation in micro-scale channels to cool microeletronic devices," *Revista de Engenharia Térmica*, vol. 6, no. 2, pp. 34–39, 2007.

[5] A. Joy, K. Shiblemon, and B. Baby, "Review on fabrication and experimental study of microchannel heat sinks for cooling of electronic components," *Materials Today: Proceedings*, vol. 72, pp. 2985–2991, 2023.

[6] "Intel ships pentium® 4 processor operating at 2.2 billion cycles per second." https://www.intel.com/pressroom/archive/releases/2002/20020107comp.htm. (Accessed on 02/14/2024).

[7] L. Zhang, K. E. Goodson, and T. W. Kenny, *Silicon microchannel heat sinks: theories and phenomena*. Springer Science & Business Media, 2004.

[8] H.-M. Tong, Y.-S. Lai, and C. Wong, *Advanced flip chip packaging*, vol. 142. Springer, 2013.

[9] P. Bhandari, K. S. Rawat, Y. K. Prajapati, D. Padalia, L. Ranakoti, and T. Singh, "Design modifications in micro pin fin configuration of microchannel

heat sink for single phase liquid flow: A review," *Journal of Energy Storage*, vol. 66, p. 107548, 2023.

[10] C. Perret, C. Schaeffer, and J. Boussey, "Microchannel integrated heat sinks in silicon technology," in *Conference Record of 1998 IEEE Industry Applications Conference. Thirty-Third IAS Annual Meeting (Cat. No. 98CH36242)*, vol. 2, pp. 1051–1055, IEEE, 1998.

[11] H. Wang, Z. Chen, and J. Gao, "Influence of geometric parameters on flow and heat transfer performance of micro-channel heat sinks," *Applied Thermal Engineering*, vol. 107, pp. 870–879, 2016.

[12] A. Alfaryjat, H. Mohammed, N. M. Adam, M. Ariffin, and M. I. Najafabadi, "Influence of geometrical parameters of hexagonal, circular, and rhombus microchannel heat sinks on the thermohydraulic characteristics," *International Communications in Heat and Mass Transfer*, vol. 52, pp. 121–131, 2014.

[13] X.-Q. Wang, A. S. Mujumdar, and C. Yap, "Thermal characteristics of tree-shaped microchannel nets for cooling of a rectangular heat sink," *International Journal of Thermal Sciences*, vol. 45, no. 11, pp. 1103–1112, 2006.

[14] G. Xia, L. Chai, H. Wang, M. Zhou, and Z. Cui, "Optimum thermal design of microchannel heat sink with triangular reentrant cavities," *Applied Thermal Engineering*, vol. 31, no. 6-7, pp. 1208–1219, 2011.

[15] Q. Zhu, K. Chang, J. Chen, X. Zhang, H. Xia, H. Zhang, H. Wang, H. Li, and Y. Jin, "Characteristics of heat transfer and fluid flow in microchannel heat sinks with rectangular grooves and different shaped ribs," *Alexandria Engineering Journal*, vol. 59, no. 6, pp. 4593–4609, 2020.

[16] D. Zhuang, Y. Yang, G. Ding, X. Du, and Z. Hu, "Optimization of microchannel heat sink with rhombus fractal-like units for electronic chip cooling," *International Journal of Refrigeration*, vol. 116, pp. 108–118, 2020.

[17] J. Li and G. Peterson, "Geometric optimization of a micro heat sink with liquid flow," *IEEE Transactions on Components and Packaging Technologies*, vol. 29, no. 1, pp. 145–154, 2006.

[18] Y. K. Prajapati, "Influence of fin height on heat transfer and fluid flow characteristics of rectangular microchannel heat sink," *International Journal of Heat and Mass Transfer*, vol. 137, pp. 1041–1052, 2019.

[19] G. Gamrat, M. Favre-Marinet, and D. Asendrych, "Conduction and entrance effects on laminar liquid flow and heat transfer in rectangular microchannels," *International Journal of Heat and Mass Transfer*, vol. 48, no. 14, pp. 2943–2954, 2005.

[20] A. Koşar, "Effect of substrate thickness and material on heat transfer in microchannel heat sinks," *International Journal of Thermal Sciences*, vol. 49, no. 4, pp. 635–642, 2010.

[21] H.-C. Chiu, J.-H. Jang, H.-W. Yeh, and M.-S. Wu, "The heat transfer characteristics of liquid cooling heatsink containing microchannels," *International Journal of Heat and Mass Transfer*, vol. 54, no. 1-3, pp. 34–42, 2011.

[22] A. Abdoli, G. Jimenez, and G. S. Dulikravich, "Thermo-fluid analysis of micro pin-fin array cooling configurations for high heat fluxes with a hot spot," *International Journal of Thermal Sciences*, vol. 90, pp. 290–297, 2015.

[23] H. M. Ali and W. Arshad, "Thermal performance investigation of staggered and inline pin fin heat sinks using water based rutile and anatase tio2 nanofluids," *Energy conversion and management*, vol. 106, pp. 793–803, 2015.

[24] N. Guan, T. Luan, G. Jiang, Z.-G. Liu, and C.-W. Zhang, "Influence of heating load on heat transfer characteristics in micro-pin-fin arrays," *Heat and Mass Transfer*, vol. 52, pp. 393–405, 2016.

[25] D. Ansari and K.-Y. Kim, "Hotspot thermal management using a microchannel-pinfin hybrid heat sink," *International Journal of Thermal Sciences*, vol. 134, pp. 27–39, 2018.

[26] D. Ansari and K.-Y. Kim, "Hotspot management using a hybrid heat sink with stepped pin-fins," *Numerical Heat Transfer, Part A: Applications*, vol. 75, no. 6, pp. 359–380, 2019.

[27] P. Bhandari and Y. K. Prajapati, "Fluid flow and heat transfer behavior in distinct array of stepped micro-pin fin heat sink," *Journal of Enhanced heat transfer*, vol. 28, no. 4, 2021.

[28] P. Bhandari, Y. K. Prajapati, and A. Uniyal, "Influence of three dimensionality effects on thermal hydraulic performance for stepped micro pin fin heat sink," *Meccanica*, vol. 58, no. 11, pp. 2113–2129, 2023.

[29] P. Bhandari, D. Padalia, L. Ranakoti, R. Khargotra, K. András, and T. Singh, "Thermo-hydraulic investigation of open micro prism pin fin heat sink having varying prism sides," *Alexandria Engineering Journal*, vol. 69, pp. 457–468, 2023.

[30] H.-C. Chiu, R.-H. Hsieh, K. Wang, J.-H. Jang, and C.-R. Yu, "The heat transfer characteristics of liquid cooling heat sink with micro pin fins," *International communications in heat and mass transfer*, vol. 86, pp. 174–180, 2017.

[31] D. Cooke and S. G. Kandlikar, "Effect of open microchannel geometry on pool boiling enhancement," *International Journal of Heat and Mass Transfer*, vol. 55, no. 4, pp. 1004–1013, 2012.

[32] D. Deng, L. Zeng, and W. Sun, "A review on flow boiling enhancement and fabrication of enhanced microchannels of microchannel heat sinks," *International Journal of Heat and Mass Transfer*, vol. 175, p. 121332, 2021.

[33] M. I. Hasan, "Investigation of flow and heat transfer characteristics in micro pin fin heat sink with nanofluid," *Applied thermal engineering*, vol. 63, no. 2, pp. 598–607, 2014.

[34] J. Hua, G. Li, X. Zhao, and Q. Li, "Experimental study on thermal performance of micro pin fin heat sinks with various shapes," *Heat and mass transfer*, vol. 53, pp. 1093–1104, 2017.

[35] J. Hua, G. Li, X. Zhao, Q. Li, and J. Hu, "Study on the flow resistance performance of fluid cross various shapes of micro-scale pin fin," *Applied thermal engineering*, vol. 107, pp. 768–775, 2016.

[36] T. İzci, M. Koz, and A. Koşar, "The effect of micro pin-fin shape on thermal and hydraulic performance of micro pin-fin heat sinks," *Heat Transfer Engineering*, vol. 36, no. 17, pp. 1447–1457, 2015.

[37] T. John, B. Mathew, and H. Hegab, "S-shaped pin-fins for enhancement of overall performance of the pin-fin heat sink," in *Fluids Engineering Division Summer Meeting*, vol. 49484, pp. 1717–1725, 2010.

[38] F. Keshavarz, A. Mirabdolah Lavasani, and H. Bayat, "Numerical analysis of effect of nanofluid and fin distribution density on thermal and hydraulic performance of a heat sink with drop-shaped micropin fins," *Journal of Thermal Analysis and Calorimetry*, vol. 135, pp. 1211–1228, 2019.

[39] A. K. Sadaghiani and A. Koşar, "Numerical investigations on the effect of fin shape and surface roughness on hydrothermal characteristics of slip flows in microchannels with pin fins," *International Journal of Thermal Sciences*, vol. 124, pp. 375–386, 2018.

[40] G. V. Kewalramani, G. Hedau, S. K. Saha, and A. Agrawal, "Study of laminar single phase frictional factor and nusselt number in in-line micro pin-fin heat sink for electronic cooling applications," *International Journal of Heat and Mass Transfer*, vol. 138, pp. 796–808, 2019.

[41] M. Khoshvaght-Aliabadi, S. Deldar, and S. Hassani, "Effects of pin-fins geometry and nanofluid on the performance of a pin-fin miniature heat sink (pfmhs)," *International Journal of Mechanical Sciences*, vol. 148, pp. 442–458, 2018.

[42] Y. J. Lee, P. K. Singh, and P. S. Lee, "Fluid flow and heat transfer investigations on enhanced microchannel heat sink using oblique fins with parametric study," *International Journal of Heat and Mass Transfer*, vol. 81, pp. 325–336, 2015.

[43] A. Koşar, C. Mishra, and Y. Peles, "Laminar flow across a bank of low aspect ratio micro pin fins," *Journal of Fluids Engineering*, 2005.

[44] A. Koşar and Y. Peles, "Thermal-hydraulic performance of mems-based pin fin heat sink," *ASME Journal of Heat and Mass Transfer*, 2006.

[45] A. Kosar and Y. Peles, "Tcpt-2006-096. r2: Micro scale pin fin heat sinks—parametric performance evaluation study," *IEEE Transactions on Components and Packaging Technologies*, vol. 30, no. 4, pp. 855–865, 2007.

[46] M. Liu, D. Liu, S. Xu, and Y. Chen, "Experimental study on liquid flow and heat transfer in micro square pin fin heat sink," *International Journal of Heat and Mass Transfer*, vol. 54, no. 25-26, pp. 5602–5611, 2011.

[47] Z. Liu, N. Guan, C. Zhang, and G. Jiang, "The flow resistance and heat transfer characteristics of micro pin-fins with different cross-sectional shapes," *Nanoscale and Microscale Thermophysical Engineering*, vol. 19, no. 3, pp. 221–243, 2015.

[48] D. Mei, X. Lou, M. Qian, Z. Yao, L. Liang, and Z. Chen, "Effect of tip clearance on the heat transfer and pressure drop performance in the micro-reactor with micro-pin–fin arrays at low reynolds number," *International Journal of Heat and Mass Transfer*, vol. 70, pp. 709–718, 2014.

[49] Y. Peles, A. Koşar, C. Mishra, C.-J. Kuo, and B. Schneider, "Forced convective heat transfer across a pin fin micro heat sink," *International Journal of Heat and Mass Transfer*, vol. 48, no. 17, pp. 3615–3627, 2005.

[50] R. S. Prasher, J. Dirner, J.-Y. Chang, A. Myers, D. Chau, D. He, and S. Prstic, "Nusselt number and friction factor of staggered arrays of low aspect ratio micropin-fins under cross flow for water as fluid," *ASME Journal of Heat and Mass Transfer*, 2007.

[51] B. R. Far, S. K. Mohammadian, S. K. Khanna, and Y. Zhang, "Effects of pin tip-clearance on the performance of an enhanced microchannel heat sink with oblique fins and phase change material slurry," *International Journal of Heat and Mass Transfer*, vol. 83, pp. 136–145, 2015.

[52] E. Rasouli, C. Naderi, and V. Narayanan, "Pitch and aspect ratio effects on single-phase heat transfer through microscale pin fin heat sinks," *International Journal of Heat and Mass Transfer*, vol. 118, pp. 416–428, 2018.

[53] S. R. Reddy, A. Abdoli, G. S. Dulikravich, C. C. Pacheco, G. Vasquez, R. Jha, M. J. Colaco, and H. R. Orlande, "Multi-objective optimization of micro pin-fin arrays for cooling of high heat flux electronics with a hot spot," *Heat Transfer Engineering*, vol. 38, no. 14-15, pp. 1235–1246, 2017.

[54] M. Rezaee, M. Khoshvaght-Aliabadi, A. A. Arani, and S. Mazloumi, "Heat transfer intensification in pin-fin heat sink by changing pin-length/longitudinal-pitch," *Chemical Engineering and Processing-Process Intensification*, vol. 141, p. 107544, 2019.

[55] A. Rozati, D. K. Tafti, and N. E. Blackwell, "Effect of pin tip clearance on flow and heat transfer at low reynolds numbers," *ASME Journal of Heat and Mass Transfer*, 2008.

[56] C. A. Rubio-Jimenez, S. G. Kandlikar, and A. Hernandez-Guerrero, "Numerical analysis of novel micro pin fin heat sink with variable fin density," *IEEE transactions on components, packaging and manufacturing technology*, vol. 2, no. 5, pp. 825–833, 2012.

[57] C. A. Rubio-Jimenez, S. G. Kandlikar, and A. Hernandez-Guerrero, "Performance of online and offset micro pin-fin heat sinks with variable fin density," *IEEE transactions on components, packaging and manufacturing technology*, vol. 3, no. 1, pp. 86–93, 2012.

[58] H. Shafeie, O. Abouali, K. Jafarpur, and G. Ahmadi, "Numerical study of heat transfer performance of single-phase heat sinks with micro pin-fin structures," *Applied Thermal Engineering*, vol. 58, no. 1-2, pp. 68–76, 2013.

[59] G. Singh, R. Kumar, and D. Mikielewicz, "Effect of flow normalization in micro-pin-finned heat sink: Numerical study," *Journal of Thermophysics and Heat Transfer*, vol. 35, no. 1, pp. 28–37, 2021.

[60] R. Chein and G. Huang, "Analysis of microchannel heat sink performance using nanofluids," *Applied thermal engineering*, vol. 25, no. 17-18, pp. 3104–3114, 2005.

[61] O. S. Prajapati, N. Rohatgi, *et al.*, "Flow boiling heat transfer enhancement by using zno-water nanofluids," *Science and Technology of Nuclear Installations*, vol. 2014, 2014.

[62] P. Bhandari and Y. K. Prajapati, "Thermal performance of open microchannel heat sink with variable pin fin height," *International journal of thermal sciences*, vol. 159, p. 106609, 2021.

[63] V. Yadav, K. Baghel, R. Kumar, and S. Kadam, "Numerical investigation of heat transfer in extended surface microchannels," *International Journal of Heat and Mass Transfer*, vol. 93, pp. 612–622, 2016.

[64] S. Patankar, *Numerical heat transfer and fluid flow.* CRC press, Ed.2018.